

We thank the Associate Editor for the opportunity to make revisions to our manuscript in review by *Biogeosciences*. All (three) referee's comments are in italics, our responses are in bold, and our comments to the Associate Editor are in red. Any so-called "appended figure" can be viewed in the Interactive discussion.

In order for the results to be more useful to other users I recommend that the average fluxes also be given according to different salinity ranges. The results are now given for the upper and lower estuaries as well as the gulf. Should the average fluxes be given over different salinity ranges the results would be easier to be integrated into the global carbon flux.

Given the physiography (funnel shape) and the large physical dimensions of the maritime portion of the St. Lawrence Estuary, we pursued an analysis of surface-water pCO₂ and CO₂ flux data in terms of space rather than salinity. With 75% of its total surface area occupied by the Lower Estuary (Tadoussac to Pointe-des-Monts, $S > \sim 21.2$), it is more realistic to integrate/weight the fluxes spatially than to provide average fluxes binned by salinity, in order to obtain a representative whole-estuary flux. Furthermore, as you can appreciate from the appended figure (see Fig. 1), active processes along the estuary are not as clearly defined when the data are plotted as a function of surface salinity. Whereas the plot still shows that the Upper Estuary ($S < \sim 24.5$; surface salinity fluctuations are found around the Upper-Lower Estuary boundary due to tidally-induced upwelling of salty intermediate/bottom waters) is heterotrophic, it fails to highlight the autotrophic character of the Lower Estuary and the neutral character of the Gulf, the latter being substantially larger in surface area than the combined Upper and Lower Estuaries but contributing little to the net CO₂ flux.

This is addressed by lines 672–675 in the revised manuscript.

Besides, dividing data into only three geographical regions misses an important feature. That is, the undersaturation of CO₂ between the 300-600km stretch is neither noted nor discussed. Does the undersaturation correspond to the large river plume where undersaturation is frequently found(see Chen et al., 2012)? Would dividing the data according to salinity better characterize the data?

As noted in lines 643-649, we suggest that biological production is responsible for the observed drawdown of pCO₂ in the surface waters of the Lower Estuary as well

as the undersaturation observed near the Estuary-Gulf boundary (i.e., along the 300-600 km stretch).

This is addressed by lines 924–926 in the revised manuscript.

Two minor points: The red line and the dashed black line in Fig. 9 should be identified. Line 41: the fact that the release of CO₂ from estuaries is balanced by the absorption of CO₂ from shelves was first reported by Chen and Borges(2009) prior to the two references given.

We agree with the reviewer's comment that this needs to be explicitly stated in the revised manuscript. We will identify the red (smoothed temperature data using a moving average filter with a span of 50% of the total number of data points) and dashed (smoothed pCO₂(water) data) lines in the Fig. 9 caption, and add the appropriate reference to line 41 in the revised manuscript.

This is addressed by lines 1692–1694 in the revised manuscript.

Page 2 (lines 39-40): The emissions of 0.25 Pg C yr⁻¹ proposed by Regnier et al. (2013) are based on Laruelle et al. (2010) and Cai (2011). Please include this information. See also Chen et al. (2013) and Laruelle et al. (2013), with updated values (0.10 Pg C yr⁻¹).

Laruelle et al. (2013). Global multi-scale segmentation of continental and coastal waters from the watersheds to the continental margins. Hydrol. Earth Syst. Sci., 17, 2029-2051.

We will add the appropriate reference to line 40 in the revised manuscript.

This is addressed by line 48 in the revised manuscript.

Page 2 (lines 42-43): Yes, and I agree. However, studies conducted in marine-dominated estuaries showed that they can present pCO₂ values below 400 ppmv and a sink behavior. Please, check Koné et al. (2010); Maher and Eyre (2012), Cotovicz Jr. et al (2015).

Koné et al. (2009). Seasonal variability of carbon dioxide in the rivers and lagoons of Ivory Coast (West Africa). Estuar. Coast., 32, 246-260, 2009.

Maier and Eyre (2012). Carbon budgets for three autotrophic Australian estuaries: Implications for global estimates of the coastal air-water CO₂ flux. Global Biogeochem. Cy., 26,GB1032.

Cotovicz Jr. et al. (2015). A strong CO₂ sink enhanced by eutrophication in a tropical coastal embayment (Guanabara Bay, Rio de Janeiro, Brazil). Biogeosciences, 12, 5125-6146.

Marine-dominated estuaries are briefly discussed in the Introduction in lines 91-99. Although they are underrepresented in data compilations, some behave as net CO₂ sinks. This will be explicitly stated in the revised manuscript and supported by the recommended references.

This is addressed by lines 127–129 in the revised manuscript.

Page 3 (lines 76-78): Please check Borges and Abril (2011) to see details about the drivers of the emissions of CO₂ to the atmosphere from estuaries.

Borges, A. V. and Abril, G.: Carbon Dioxide and Methane Dynamics in Estuaries, in: Treatise on Estuarine and Coastal Science, edited by: Eric, W. and Donald, M., Academic Press, Amsterdam, 119-161, 2011.

We thank the reviewer for the referral to Borges and Abril (2011). By analyzing a data set of nine European and two US estuaries, the authors concluded that 10 % of the total emission of CO₂ from inner estuaries could be attributed to the ventilation of riverine CO₂, whereas 90 % of the emission could be attributed to net heterotrophy. These two main drivers of estuarine CO₂ degassing are noted in lines 76-80 of this manuscript. Borges and Abril (2011) also detailed the relationship between freshwater residence time and the relative contribution of riverine CO₂ ventilation. This will be addressed in the revised manuscript.

This is addressed by lines 99–101 in the revised manuscript.

Page 3 (lines 91-95): I think that the most overlooked estuarine typology regarding CO₂ emissions are the marine-dominated estuaries.

We agree with the reviewer on this point.

This is addressed by line 115 in the revised manuscript.

Page 4 (lines 119-121): I would like to know about the wintertime period. Did you perform sampling campaigns at this period? Could you give some discussion about this?

With the exception of the 2016 cruise, water samples used in this work were obtained opportunistically on research cruises conducted during the spring and summer seasons. The Estuary and the Gulf are typically covered by ice during the winter months. Coast Guard icebreakers keep shipping lanes open during the winter, but, even though we have been offered berths onboard, the icebreakers will not stop for discrete water sampling. Hence, there is no data for the winter season. We have recently submitted, under a newly-created program, a multimillion-dollar proposal that would provide us with dedicated time on an icebreaker during the wintertime and, possibly, a vessel (CCGS Amundsen) equipped with an underway pCO₂ system.

This is addressed by line 278 in the revised manuscript.

Page 6 (lines 202-203): And also vertically, not?

The Upper Estuary is strongly laterally stratified, but because it is generally shallow and, due to the turbulence generated by tides, winds, and waves interacting with the bottom topography, it is only very slightly vertically stratified. In contrast, the Lower Estuary, because it is much deeper, is strongly vertically stratified. See the appended Fig. 1.

This is addressed by line 257 in the revised manuscript.

Page 7 (lines 225-228): Please, provide more details about the sampling strategy. What is the vertical resolution (water column) of the sampling? How many samples did you take each year? How many samples did you take adding all campaigns?

As the present work focuses on the inorganic carbon chemistry of the surface mixed layer, the total number of surface-water samples (N) taken from the River, Upper Estuary, Lower Estuary, and Gulf are summarized in Table 2. Nevertheless, in all cases the whole water column was sampled, typically at 3 m, 20 m, 50 m, 70 m, 100 m and at 50m intervals to the bottom (or within 10 m of the bottom). These data will be presented in a subsequent manuscript in which the geochemical and isotopic

characteristics of source-water masses and their relative contributions to the Estuary will be examined.

This is addressed by lines 279–283 in the revised manuscript.

Page 8 (lines 240-244): Did you filter the water for the total alkalinity measurements? Previous works showed that for coastal waters the phytoplankton and bacterial cells can affect the measured alkalinity of unfiltered samples (Kim et al. 2006; Chanson and Millero, 2007). Do you have information about the particulate inorganic content (e.g., CaCO₃) of the sampled waters? Please, see Kim et al. (2006) and Chanson and Millero (2007) about this problematic.

Kim et al. (2006). Contribution of phytoplankton and bacterial cells to the measured alkalinity of seawater. Limnol. Oceanogr. 51 (1), 331-338.

Chanson and Millero (2007). Effect of filtration on the total alkalinity of open-ocean seawater. Limnol. Oceanogr.: Methods 5, 293-295.

The sampling protocol we used is standard for TAlk and DIC measurements in open ocean waters (Dickson and Goyet, 1994). Hence, our samples were not filtered, but when SPM concentrations were high (in the turbidity maximum of the Upper Estuary), the SPM was allowed to settle for several days before the supernatant was sampled for analysis. Previous experiments with filtered and unfiltered samples revealed that results were identical within the analytical uncertainty ($\pm 2 \mu\text{mol/kg}$) of our measurements.

The phytoplankton community composition in the study area is strongly dominated by diatoms (Devine et al., 2015). There is no significant population of pelagic carbonate-secreting organisms (coccolithophores, foraminifera, pteropods) in the St. Lawrence Estuary and Gulf. *Emiliana huxleyi* (coccolithophore) can be found at relatively low concentrations (maximum of $\sim 10^7$ coccoliths/L) in the upper mixed layer in the Gulf and in the Strait of Belle Isle, while small specimens of *Limacina helicina* (pteropod) have been found in very low abundance (maximum of 18 individuals/m²) in the Strait and in the Gulf (Levasseur et al., 1994; Cantin et al., 1996; Levasseur et al., 1997). Detrital carbonates are eroded from the Silurian-Ordovician deposits of Anticosti Island in the Gulf, but our sampling was carried out far from the source.

Dickson, A. G. and Goyet, C. (Eds.): Handbook of Methods for the Analysis of the Various 800 Parameters of the Carbon Dioxide System in Sea Water (Version 2), U.S. Department of Energy, 801 ORNL/CDIAC-74, 1994.

Devine, L., Plourde, S., Starr, M., St-Pierre, J.-F., St-Amand, L., Joly, P., and Galbraith, P. S.: Chemical and biological oceanographic conditions in the Estuary and Gulf of St. Lawrence during 2013, DFO Can. Sci. Advis. Sec. Res. Doc., 2015/013, 45 pp., 2015.

Levasseur, M., Keller, M. D., Bonneau, E., D'Amours, D., and Bellows, W. K.: Oceanographic basis of a DMS-related Atlantic cod (*Gadus morhua*) fishery problem: blackberry feed, Can. J. Fish. Aquat. Sci., 51, 881–889, 1994.

Cantin, G., Levasseur, M., Gosselin, M., and Michaud, S.: Role of zooplankton in the mesoscale distribution of surface dimethylsulfide concentrations in the Gulf of St. Lawrence, Canada, Mar. Ecol.-Prog. Ser., 141, 103–117, 1996.

Levasseur, M., Sharma, S., Cantin, G., Michaud, S., Gosselin, M., and Barrie, L.: Biogenic sulfur emissions from the Gulf of Saint Lawrence and assessment of its impact on the Canadian east coast, J. Geophys. Res.-Atmos., 102, 28025–28039, 1997.

This is addressed only in the Interactive discussion.

Page 10 (lines-315-327): This paragraph is confused. As you said before "The samples were taken at 3 m...", then why no use this depth for the individual data points of surface-water pCO₂ at each sampling location? It is not clear what data were averaged.

For each sampling station, data points in the surface mixed layer (SML), which exchanges heat and gases (e.g., CO₂) with the overlying atmosphere, were averaged. Given limited sampling in surface waters above the cold intermediate layer, the mixed-layer dataset at each station was most often limited to a single sample (from ~2 or ~3m depth), although, in a few cases, it included a sample taken at ~10m depth.

This is addressed by lines 281–283 in the revised manuscript.

Page 10-11 (lines 331-348): This is an important section showing that your results at the low salinity region (0-5) can be overestimated or underestimated. This depends of the formulations of K_1 and K_2 . Could you give more details about this? Did you perform direct $p\text{CO}_2$ measurements to compare results? What values of pH and TAlk did you use for the Figure 3? Please include this information in the figure caption.

As noted in lines 301-306, the $p\text{CO}_2$ values used in this work were calculated from the measured pH and TAlk, using the carbonic acid dissociation constants, K_1 and K_2 , of Cai and Wang (1998). Whereas we have occasionally carried out DIC measurements on the water samples, direct $p\text{CO}_2$ measurements were not carried out as we do not have access to the proper equipment. We agree with the reviewer that direct $p\text{CO}_2$ measurements would have been desirable to confirm the accuracy of the $p\text{CO}_2$ calculations.

An underway $p\text{CO}_2$ system (General Oceanics model 8050) was operated by a colleague at the University of Manitoba, Prof. Tim Papakyriakou, and his students on the Canadian Coast Guard Ship (CCGS) and icebreaker Amundsen as it made its way through the Gulf of St. Lawrence to the Arctic for a scientific survey in early June 2016. Unfortunately, although the vessel left from its port-of-call in Québec City, the system was not turned on until well into the Gulf of St. Lawrence (near Anticosti Island) and through the Strait of Belle Isle. When in operation, the system was continuously sampling water from a high-volume inlet located at a depth of 5 m. Water was cycled through the underway system at a rate of $2.4 - 2.8 \text{ L min}^{-1}$ and calibrations of the system's infrared gas analyzer (LI-COR model LI-7000) were monitored twice daily against three certified gas standards traceable to WMO standards. The underway system has an expected accuracy of $2 \mu\text{atm}$ (Pierrot et al., 2009). The underway $p\text{CO}_2$ measurements near Anticosti Island were in good agreement with the $p\text{CO}_2$ calculated in this study, for neighboring locations sampled in May 2016 aboard the RV Coriolis II (see the appended Fig. 2). Measured and calculated $p\text{CO}_2$ differed by, on average, $\sim 4.2 \%$.

For the comparison of dissociation constants (results presented in Figure 3), values of $p\text{CO}_2$ were calculated at a constant temperature of $15 \text{ }^\circ\text{C}$, at the measured pH and TAlk, using different published formulations of K_1 and K_2 : Cai and Wang (1998), Lueker et al. (2000), Roy et al. (1993), Millero (2010), and Millero (1979) for pure water only. This is noted in the Figure 3 caption, lines 1163-1167.

Pierrot, D., C. Neill, K. Sullivan, R. Castle, R. Wanninkhof, H. Lüger, T. Johannessen, A. Olsen, R. A. Feely, and C. E. Cosca (2009), Recommendations for autonomous

underway pCO₂ measuring systems and data-reduction routines, Deep. Res. Part II, 56(8-10), 512-522, doi:10.1016/j.dsr2.2008.12.005.

This is addressed by lines 382–383, 422–424, and 1617–1621 in the revised manuscript.

Page 11 (lines 362-363) and Page 12 (lines 385): Could you describe the methodology for DIC analyses?

As noted in lines 301-306, most DIC values were calculated from the measured pH and TAlk, using the K₁ and K₂ of Cai and Wang (1998). These calculated DIC values, along with the measured TAlk, were used to temperature-normalize the pCO₂, according to the method of Jiang et al. (2008).

Direct DIC measurements were carried out during the 2014 cruise using a Scitech Apollo DIC analyzer. After being thermostated at 25 °C, 1–1.5 mL of the sample was injected into the instrument's reactor where it was acidified with 10 % H₃PO₄ and the evolved CO₂ carried by a stream of pure nitrogen to a LICOR infrared analyzer. A calibration curve was constructed using gravimetrically-prepared Na₂CO₃ solutions, and the accuracy of the measurements was verified using certified reference material solutions provided by Andrew Dickson (Scripps Institute of Oceanography). The reproducibility of the measurements was typically on the order of 0.2 %. Results of the direct DIC and pH measurements were used to assess the contribution of organic alkalinity to the total alkalinity in the Upper Estuary. The latter was found to be negligible (~20 μmol/kg) relative to TAlk within the freshwater end-member (St. Lawrence River) and decreased seaward with increasing salinity along the Upper Estuary. Hence, measured and calculated DIC values were compatible. The DIC analytical methodology will be added to the revised manuscript.

This is addressed by lines 342–351 in the revised manuscript.

Page 14 (lines 466-474): Do you think that hourly wind speed data averaged over the sampling month is a good approach to obtain a transfer velocity? Did you compare the hourly data average with other approach (minute/10minutes average wind speed) to investigate differences?

As the wind speed data used in this work were obtained from an external source (Environment Canada), we were limited to the data intervals of hourly, daily, or

monthly. Average hourly wind speed data served as our best proxy for the steady (short-term) wind speed required by the equation of Wanninkhof (lines 460-461), which is applicable to estimate the gas transfer velocity from instantaneous wind speed measurements, using, for example, shipboard anemometers. The wind speeds provided by Environment Canada are observed from an anemometer.

It should be noted that shipboard measurements of instantaneous wind speed were available from the ship's log, but only for a limited number of stations from the 2010 and 2013 cruises. We elected to use the historical hourly weather data from Environment Canada for two reasons: (1) the data was more complete across time, and (2) the location of observing stations was consistent across space.

This is addressed only in the Interactive discussion.

Pages 15 and 16 (section 2.6): The approach of Carrillo et al. (2004) is a good way to compare the distributions and controls of biologically reactive dissolved gases. However, I also suggest compare the Apparent Oxygen Utilization (AOU) (Benson and Krause, 1984) with the Excess of DIC (E-DIC) (Abril et al 2003) that was applied in wide typologies of estuarine systems (e. g., Borges and Abril, 2011). Maybe you can compare the two approaches.

The DO percent saturation (%DO(sat)) values used in this study were calculated as: $\%DO(sat) = DO/DO^* \times 100$, where DO is the measured DO and DO* is the equilibrium DO computed from the equation of Benson and Krause (1984). Similarly, AOU is defined as: $AOU = DO^* - DO$. Hence, we would expect the two approaches to yield similar results, and, in fact, they do, with the majority of data from the Upper Estuary showing the signature of respiration and the majority of data from the Lower Estuary and Gulf showing photosynthesis. See the appended Fig. 3.

This is addressed by lines 722–726 and by the updated Fig. 8 in the revised manuscript.

Page 17 (lines 559-568): Do you have results of chlorophyll a concentrations? Do you have the results of column water stratification at this region? It's clear that the region of SLE near Pointe-des-Monts (between Tadoussac and Anticosti Island) present the pCO₂ values lower than atmospheric pCO₂ for all sampling campaigns. I think that some results of chlorophyll a and/or primary production could better support your discussion. I think you should include more discussion.

Whereas direct measurements of chlorophyll-a concentrations were not carried out during the research cruises, a fluorescence sensor was mounted on the CTD probe. Maximum fluorescence values measured in the euphotic zone at each sampling station are shown in the appended Fig. 4. Mean values of transmission (% light transmission) are also shown in Fig. 4. Low transmission values are due to light absorption by suspended particulate matter and colored dissolved organic matter, the latter being negligible in our study area. The maximum fluorescence values, along with high transmission values approaching 100%, were observed in the eastern Lower Estuary and western Gulf, where the system shifts from net heterotrophy to net autotrophy. Hence, these data further support our original interpretations.

The water column is strongly stratified in the Lower Estuary and the Gulf, which enhances biological production as discussed in lines 560-566. See the appended Fig. 1 for vertical profiles of temperature and salinity.

This is addressed by lines 985–990 in the revised manuscript.

Page 17 and 18 (lines 570-580): Could you give comparisons with other studies?

Hunt et al. (2014) indicate that temperature variability is one of the major controlling factors of seasonal changes in pCO₂ in the Kennebec Estuary, a large, river-dominated, macrotidal estuary. Had we been able to assess the temporal variability of pCO₂ in the St. Lawrence Estuary throughout the year (e.g., from summer to winter), we would expect that temperature exerts more control on the pCO₂ changes, due to larger seasonal temperature variability as well as the absence of phytoplankton blooms in winter.

This is addressed only in the Interactive discussion.

Page 18 (lines 606-608): Previous studies identified CO₂ sink behavior in estuaries. Please see Koné et al (2010); Maher and Eyre (2012); Cotovicz Jr et al (2015).

We thank the reviewer for bringing these studies to our attention as they demonstrate that some estuarine systems (e.g., those characterized by strong stratification and/or marine dominance) behave as net CO₂ sinks rather than CO₂ sources. We will refer to these studies in the revised manuscript.

This is addressed by lines 128–130 in the revised manuscript.

Page 18 and 19 (Section 3.2): Please, provide comparisons of CO₂ fluxes with other studies. Could you identify in the Figure 1 (or other) each segment considered in this study to the calculations of the area-averaged air-sea CO₂ fluxes?

We agree with the reviewer's comment that the segmentation of the Estuary for the calculation of the area-averaged CO₂ flux should be shown on a map of the study area. See the appended Fig. 5, which will be used in the revised manuscript.

This is addressed by lines 1570–1571 in the revised manuscript.

Page 19 (lines 628-631): The biological activity can also drawdown the DIC concentrations in water column.

Photosynthesis is mentioned in line 628, but we agree with the reviewer's comment that the biological removal of DIC could be explicitly stated in line 629.

This is addressed by line 910 in the revised manuscript.

Page 20 (lines 645-651): In this section you can find other estuaries that acts as CO₂ sink. Also, I think you could search in literature other papers that compared the biological x temperature effects over pCO₂ concentrations to better contextualize you work (Bozec et al.,2011; Zhang et al., 2012; Hunt et al., 2014; Cotovicz Jr et al., 2015).

Bozec et al. (2011). Diurnal to inter-annual dynamics of pCO₂ recorded by a CARIOCA sensor in a temperate coastal ecosystem (2003-2009). Mar. Chem., 126, 13-26.

Zhang et al. (2012). Distribution and seasonal variation in the partial pressure of CO₂ during autumn and winter in Jiaozhou Bay, a region of high urbanization. Mar. Pollut. Bull., 64, 56-65.

Hunt et al. (2014). CO₂ Input Dynamics and Air-Sea Exchange in a Large New England Estuary. Estuar. Coast., 37, 1078-1091.

The relative importance of physical and biological controls on spatial variations of surface-water pCO₂ in the St. Lawrence Estuary will be more rigorously examined in

a follow-up manuscript, by applying a quantitative water-mass analysis to remove the effect of physical mixing on the pCO₂ observations.

This is addressed by lines 914–916 in the revised manuscript.

Figure 4: Could you move the legend of Figure 4 to outside the graph? Some points in the graph are over the lines of the axis. I suggest increase the ranges of the axis to put these points totally inside the graph. Also, it's evident that the GSL was sub-sampled compared to the USLE and LSLE regions. I think that it's important write about this in the methodological and discussion sections.

We agree with the reviewer's comment that the legend should be moved outside of the graph for improved readability, and the x-axis extended to encompass all data points.

The Gulf is sub-sampled in comparison to the Estuary because it is so large (~240,000 km² to the Estuary's ~12,820 km²) and exhibits less variability.

This is addressed by the updated Fig. 4 in the revised manuscript.

Figure 9: Some points in the graph are over the lines of the axis. I suggest increase the ranges of the axis to put these points totally inside the graph.

We agree with the reviewer's comment that the x-axis should be extended to encompass all data points.

This is addressed by the updated Fig. 9 in the revised manuscript.

Table 3: I am not sure that the segments that you used to calculate the air-sea CO₂ fluxes was the better division. Other graphs showed the results separated in river, upper, lower and gulf regions and maybe you can present the fluxes according.

The Estuary was divided into five equal segments to obtain a representative spatially-integrated whole-estuary CO₂ flux. Given that the Lower Estuary (Tadoussac to Pointe-des-Monts) occupies ~75 % of the total estuarine surface area, and encompasses a fairly wide range of pCO₂ values (standard deviation of 117 μatm), we decided to segment by longitude rather than salinity to, more realistically, area-normalize the sectional fluxes (see Fig. 5).

This is addressed by lines 675–678 in the revised manuscript.

1: In the introduction and later in the paper a further processes may be mentioned regulating the pCO₂ in estuarine systems. This is the relation or ratio of dissolved inorganic carbon and alkalinity (DIC:AT) of the riverine waters, which in essence is controlled by the drainage basin characteristics. This has been shown for example for the Baltic Sea by Thomas and Schneider (1999), or Hudson Bay by Burt et al. (2016). I think this process, or possibly its regional variability within or between drainage basins appears particularly relevant for systems, which span a range of climatic regions such as the Gulf of St Lawrence, being at the boundary between subarctic and temperate regions.

The authors implicitly refer to this point in their section 2.1 (geology of catchment area, as well as its vegetation), and I further think that this is relevant when discussing oxygen vs CO₂ saturation levels (lines 522-536, and their Fig. 8), as well as for section 3.3, which in turn more or less is focused on temperature only rather than on what is implied by equation 9.

We thank the reviewer for bringing these studies to our attention as they demonstrate that the DIC/TALK ratio influences pCO₂ changes by determining the buffer capacity of the water. One would expect the buffer capacity to vary among rivers that carry different levels of carbonate alkalinity according to the nature of the rocks being weathered within their drainage basin. Indeed, despite the contribution of the Ottawa River (the largest tributary of the St. Lawrence River) that drains through Paleozoic carbonates (Telmer and Veizer, 1999), we observe a DIC/TALK > 1.0 in the St. Lawrence River (freshwater end-member), but this ratio decreases rapidly with increasing salinity along the Upper St. Lawrence Estuary (USLE) (see the appended Fig. 1). The freshwater runoff from rivers on the north shore of the Lower St. Lawrence Estuary (LSLE) and Gulf, which drain the igneous and metamorphic rocks of the Grenville province, is characterized by DIC/TALK ≈ 1.0. The north shore rivers also carry a significant excess alkalinity, likely in the form of organic alkalinity (a negative alkalinity), due to their high soil-derived humic acid content. The contributions of these rivers to the LSLE and Gulf are typically negligible, except during the spring freshet in April–May, as demonstrated in a follow-up manuscript. This follow-up manuscript will also highlight that DIC inputs from in-situ respiration/remineralization processes (as opposed to riverine DIC inputs or air-sea gas exchange) are mainly responsible for controlling the spatial variability of mixed-layer pCO₂ in the Upper Estuary.

Telmer, K., and Veizer, J.: Carbon fluxes, pCO₂ and substrate weathering in a large northern river basin, Canada: carbon isotope perspectives, *Chemical Geology*, 159, 61–86, 1999.

This is addressed by lines 912–914 in the revised manuscript.

2: I appreciate the discussion of the uncertainty associated with the computation of the pCO₂ from alkalinity and pH. I find this - crucial part of the paper - somewhat difficult to follow. I would suggest to add a panel to Figure 3 showing different pCO₂ results themselves, and only then their differences. Also, while I am aware that the authors did not measure pCO₂ directly, possibly a short discussion could be added how the computed values compare to direct measurements, which is actually what the reader would be interested in.

The reviewer is referring to section 2.3.2. in the manuscript which offers a brief discussion of the uncertainty in the calculation of pCO₂ from the different published formulations of the carbonic acid dissociation constants (K₁ and K₂). For our comparison of dissociation constants, values of pCO₂ were calculated at a common temperature of 15 °C, at the measured pH and TAlk, using different sets of K₁ and K₂. The results presented in Fig. 3 were shown as a function of salinity in order to demonstrate that the best-practices formulations of K₁ and K₂ are not suitable for the low-salinity conditions found in estuaries (S_p < 19). Per the reviewer's suggestion, a second plot was added to Fig. 3 to show the actual calculations alongside the discrepancies in the calculated values. It should be clear from both plots in the appended Fig. 2 that agreement between the calculations is poorest at low salinities.

We agree with the reviewer that direct pCO₂ measurements would have been desirable to confirm the accuracy of the pCO₂ calculations, particularly at low salinities. An underway pCO₂ system (General Oceanics model 8050) was operated by a colleague at the University of Manitoba, Prof. Tim Papakyriakou, and his students on the Canadian Coast Guard Ship (CCGS) and icebreaker Amundsen as it made its way through the Gulf of St. Lawrence to the Arctic Ocean for a scientific survey in early June 2016. Unfortunately, although the vessel left from its port-of-call in Québec City, the system was not turned on until well into the Gulf of St. Lawrence (near Anticosti Island) and through the Strait of Belle Isle. When in operation, the system was continuously sampling water from a high-volume inlet located at a depth of 5 m. Water was cycled through the underway system at a rate of 2.4 - 2.8 L min⁻¹ and calibrations of the system's infrared gas analyzer (LI-COR model LI-7000)

were monitored twice daily against three certified gas standards traceable to WMO standards. The underway system has an expected accuracy of 2 μatm (Pierrot et al., 2009). The underway pCO_2 measurements near Anticosti Island were in good agreement with the pCO_2 values calculated in this study, for neighboring locations sampled in May 2016 aboard the RV Coriolis II (see the appended Fig. 3). Measured and calculated pCO_2 differed by, on average, $\sim 4.2\%$.

Pierrot, D., C. Neill, K. Sullivan, R. Castle, R. Wanninkhof, H. Lüger, T. Johannessen, A. Olsen, R. A. Feely, and C. E. Cosca (2009), Recommendations for autonomous underway pCO_2 measuring systems and data-reduction routines, *Deep. Res. Part II*, 56(8-10), 512- 522, doi:10.1016/j.dsr2.2008.12.005.

This is addressed by lines 1617–1621 in the revised manuscript.

3: Gulf of St Lawrence and another systems. While the river runoff into the Gulf of St Lawrence in North America is only second to the Mississippi system, its runoff is of similar magnitude than the one into the North Sea (300km³ per year, e.g Thomas et al., 2005), and about two thirds of the runoff into the Baltic Sea (500km³ per year). I furthermore think, a comparison with the well-studied Baltic Sea would be enlightening here as the Baltic is similarly located at the boundary between subarctic and temperate regions and is a (comparably) similar estuarine system.

We thank the reviewer for bringing to our attention the study describing the carbon budget of the North Sea. The authors indicate that the North Sea acts as a net CO_2 sink, absorbing $1.38 \text{ mol C m}^{-2} \text{ yr}^{-1}$ from the atmosphere (Thomas et al., 2005). The North Sea contrasts with the St. Lawrence Estuary, which outgasses 0.37 to 0.75 $\text{mol C m}^{-2} \text{ yr}^{-1}$ during the late spring and early summer (i.e., at the height of biological productivity). As noted by the reviewer, this is an interesting comparison to make as both systems are marine-dominated and seasonally stratified.

This is addressed only in the Interactive discussion.

1 **Spatial variability of surface-water pCO₂ and gas exchange in the**
2 **world's largest semi-enclosed estuarine system: St. Lawrence Estuary**
3 **(Canada)**

4
5 Ashley Dinauer¹ and Alfonso Mucci

6
7 GEOTOP and Department of Earth and Planetary Sciences, McGill University, 3450 University Street,
8 Montreal, QC H3A 0E8, Canada

9
10 ¹ Corresponding author (ashley.dinauer@mail.mcgill.ca)

11
12 **Abstract**

13
14 The incomplete spatial coverage of partial pressure of CO₂ (pCO₂) measurements
15 across estuary types represents a significant knowledge gap in current regional- and global-
16 scale estimates of estuarine CO₂ emissions. Given the limited research on CO₂ dynamics in
17 large estuaries and bay systems, as well as the sources of error in the calculation of pCO₂
18 (carbonic acid dissociation constants, organic alkalinity contribution), estimates of estuarine
19 CO₂ degassing may be overestimated. The Estuary and Gulf of St. Lawrence (EGSL) at the lower
20 limit of the subarctic region in eastern Canada is the largest estuarine system in the world, and
21 is characterized by an exceptional richness in environmental diversity. It is among the world's
22 most intensively studied estuaries, yet there are no published data on its surface-water pCO₂
23 distribution. To fill this data gap, a comprehensive dataset was compiled from direct and
24 indirect measurements of carbonate system parameters in the surface waters of the EGSL
25 during the spring or summer of 2003-2016. The calculated surface-water pCO₂ ranged from
26 435-765 μatm in the shallow, partially mixed Upper Estuary, 139-578 μatm in the deep,
27 stratified Lower Estuary, and 207-478 μatm along the Laurentian Channel in the Gulf. Overall,
28 at the time of sampling, the St. Lawrence Estuary served as a very weak source of CO₂ to the
29 atmosphere, with an area-averaged CO₂ degassing flux of 0.98 to 2.02 mmol C m⁻² d⁻¹ (0.36 to
30 0.74 mol C m⁻² yr⁻¹). A preliminary analysis of factors controlling the spatial variability of surface-
31 water pCO₂ revealed that respiration (Upper Estuary), photosynthesis (Lower Estuary), and
32 temperature (Gulf) were dominant controls.

33
34 **Keywords:**

35 Coastal ocean, Estuaries, CO₂, Carbon cycle, Air-sea CO₂ exchange, St. Lawrence Estuary, Gulf
36 of St. Lawrence, Laurentian Channel

Deleted: 1.00
Deleted: 2.06
Deleted: -
Deleted: -
Deleted: 0.37
Deleted: 0.75
Deleted: -
Deleted: -
Deleted: s
Deleted: are

47

48 1. Introduction

49

50 Although estuaries occupy a very small fraction (0.2 %) of the global ocean
51 surface area, their CO₂ emissions are disproportionately large compared with CO₂
52 exchanges between the open ocean and the atmosphere (Bauer et al., 2013). With an
53 estimated global efflux of 0.10-0.15 Pg C yr⁻¹ (Chen et al., 2013; Laruelle et al., 2013),
54 estuarine CO₂ degassing is thought to counterbalance CO₂ uptake on the continental
55 shelves (Chen and Borges, 2009; Laruelle et al., 2010; Cai, 2011). Almost every estuary
56 on Earth, for which data are available, is generally supersaturated with CO₂ with respect
57 to the atmosphere (Cai and Wang, 1998; Frankignoulle et al., 1998; Borges, 2005;
58 Borges et al., 2005; Borges et al., 2006; Chen and Borges, 2009; Laruelle et al., 2010;
59 Cai, 2011; Chen et al., 2012; Bauer et al., 2013; Chen et al., 2013; Regnier et al., 2013),
60 with CO₂ partial pressures (pCO₂) ranging from 400 to 10,000 µatm (in contrast, the
61 atmospheric pCO₂ in coastal zones was approximately 360–385 µatm in year 2000)
62 (Cai, 2011). Although estuaries are generally net sources of CO₂, there is considerable
63 variability and uncertainty in estimates of their CO₂ emissions, reflecting the limited
64 spatial and temporal coverage of pCO₂ measurements in estuaries as well as their
65 heterogeneous nature (hydrological and geomorphological differences, differences in
66 magnitude and stoichiometry of carbon and nutrient inputs) (Bauer et al., 2013;
67 Regnier et al., 2013).

68

69 Estuaries are geochemical reaction vessels through which continentally
70 weathered organic matter and inorganic nutrients must pass to enter the coastal ocean
71 (Kaul and Froelich, 1984). Horizontal transport is controlled by a set of physical
72 attributes (tides, wind, bathymetry, basin geography, river flow) that determine the
73 estuarine filter function (Cloern, 2001). The longer the freshwater flushing (or turnover)
74 time of the estuary, the more opportunity there is for water-column biological activity,
75 benthic exchanges and particle-dissolved phase interactions to influence its
76 biogeochemistry (Statham, 2012). DIC enrichments and pCO₂ supersaturations
77 observed in estuaries can be mainly attributed to the *in situ* microbial degradation of
78 internally and externally supplied organic carbon and the lateral transport of inorganic
79 carbon from rivers, coastal wetlands and ground waters (Bauer et al., 2013).

80

Deleted: 0.25 ± 0.25

Deleted: -

Deleted: Regnier et al., 2013

Deleted: values of partial pressure of

Deleted:

Deleted: The

Deleted: high

Deleted: pCO₂

Deleted: results from

90 In strongly tidal (macrotidal) systems, long water and particle residence times
91 (on the order of weeks to months; Middelburg and Herman, 2007) allow for the
92 extensive modification and degradation of particulate organic carbon during estuarine
93 transport (Borges et al., 2006; Chen and Borges, 2009). In the absence of seasonal or
94 permanent water stratification, the decoupling between production and degradation
95 of organic matter at and below the surface, respectively, does not occur, resulting in
96 less efficient export of dissolved inorganic carbon (Borges, 2005). Strongly tidal
97 estuaries also tend to exhibit lower levels of photosynthetic activity (Monbet, 1992) and
98 carry greater suspended particulate matter loads within their high-turbidity regions
99 (Uncles et al., 2002; Middelburg and Herman, 2007) where in suspended particles and
100 organic-rich aggregates serve as "hot spots" of microbial recycling (Statham, 2012).
101 Field measurements suggest that 10 % of the total CO₂ emissions from the inner
102 estuary of macrotidal systems is sustained by the ventilation of riverine CO₂, whereas
103 90 % is due to local net heterotrophy (Borges et al., 2006) fueled by inputs of terrestrial
104 and riverine-algae derived (planktonic) detritus and, in populated areas, sewage (Chen
105 and Borges, 2009). In estuaries with long freshwater residence times, the riverine CO₂
106 will be fully ventilated to the atmosphere within the estuary, and the total CO₂
107 emissions can be attributed to net heterotrophy (Borges and Abril, 2011).
108

109 North American estuaries rank first in terms of global estuarine surface area (41
110 %) but account for the lowest numerically averaged CO₂ flux per unit area (12 %)
111 among all continents (Chen et al., 2013). These estimates are subject to large
112 uncertainties due to data paucity. A recent synthesis by Regnier et al. (2013)
113 highlighted the meagre spatial coverage of estuarine pCO₂ measurements,
114 particularly along the Canadian eastern seaboard. Ironically, the Estuary and Gulf of St.
115 Lawrence (EGSL) in eastern Canada is the largest semi-enclosed estuarine system in
116 the world, and is among the world's most intensively studied estuaries (El-Sabh and
117 Silverberg, 1990), but was left unmentioned in recent global (Cai, 2011; Chen et al.,
118 2012; Chen et al., 2013) and regional (Laruelle et al., 2015) data compilations.
119 Furthermore, previous estuarine CO₂ studies have focused on small river-dominated
120 estuaries, whereas there has been limited research on CO₂ dynamics in large estuaries
121 and bays (Joesoef et al., 2015), i.e., marine-dominated systems, including the areas of
122 mixing at sea (outer estuaries or river plumes) (Borges et al., 2005). A comparative
123 study by Jiang et al. (2008) revealed large differences in CO₂ degassing between non-

Deleted:

Deleted: have

Deleted: concentrations

Deleted:

Deleted: s

Deleted: the majority of

Deleted: -scale

Deleted: systems

Deleted: s

Deleted: marine-

134 riverine and river-dominated estuaries and, more recently, Koné et al. (2009), Maher
135 and Eyre (2012) and Cotovicz Jr. et al. (2015) reported small CO₂ uptake by strongly
136 stratified and/or marine-dominated systems. On the U.S. east coast, the ratio of non-
137 riverine (flushed by tidal action and receiving minimum freshwater inputs) to river-
138 dominated estuaries is nearly 1:1, demonstrating the geographic importance of
139 coastal estuaries/bays on the eastern seaboard of North America (Cai, 2011).

Deleted: dominated

Deleted: while several authors note that outer estuaries (plumes) can differ substantially from inner (inland) estuaries in terms of CO₂ emissions (Frankignoulle et al., 1998; Borges, 2005; Chen et al., 2012).

140
141 The large-scale (width often considerably greater than the internal Rossby
142 radius; Cyr et al., 2015), macrotidal (mean tidal range greater than 2-4 m; Monbet,
143 1992) St. Lawrence Estuary is an excellent analogue of marine-dominated systems.
144 Throughout its length, the full spectrum of oceanic variability can be found (Mertz and
145 Gratton, 1990). Moreover, the basin characteristics and water transport time scales of
146 the St. Lawrence Estuary provide an almost ideal natural laboratory for geochemical
147 studies. Its surface waters have a renewal time of several months while its bottom
148 waters take several years to replenish, allowing for a comparison of spatial-temporal
149 variations in physical and chemical properties (El-Sabh and Silverberg, 1990). Given its
150 bimodal bathymetry, the St. Lawrence Estuary also permits the investigation of
151 biogeochemical processes in two types of estuary: (1) the shallow, partially mixed
152 Upper Estuary where physical mixing and abiotic processes dominate, and (2) the
153 deep, stratified Lower Estuary where biological cycling and oceanic processes prevail
154 (Yeats, 1990). As yet, no systematic study of the CO₂ dynamics in the St. Lawrence has
155 been published and, hence, the present study provides the first comprehensive
156 description of its mixed-layer carbonate chemistry, including (1) a multi-year
157 compilation of springtime and summertime pCO₂ calculated from direct
158 measurements of pH and alkalinity; (2) an area-averaged estimate of the air-sea CO₂
159 gas flux; and (3) an analysis of the relative importance of thermodynamic (temperature)
160 and biological (photosynthesis, respiration) processes in controlling the spatial
161 variability of surface-water pCO₂.

Deleted: the

Deleted: surface-water p

Deleted: distribution

Deleted: inorganic carbon

Deleted: field

Deleted: and pH

Deleted: estuarine

163 2. Materials and methods

164

165 2.1. Study area—St. Lawrence Estuary and Gulf

166

180 The greater St. Lawrence system (Fig. 1) connects the chain of Great Lakes, the
181 second largest terrestrial freshwater reservoir in the world, to the Atlantic Ocean (Yang
182 et al., 1996). With a drainage basin of approximately 1.32 million km², the St. Lawrence
183 River channels the second largest freshwater discharge (11,900 m³ s⁻¹) on the North
184 American continent, second only to that of the Mississippi (El-Sabh and Silverberg,
185 1990). The catchment area geology is dominated by silicate rocks of the Precambrian
186 Shield and carbonates of the Paleozoic lowlands, whose components influence the
187 downstream evolution of river chemistry (Yang et al., 1996). The erosion of the
188 carbonate rocks of the drainage basin is practically constant, as the quantity of
189 bicarbonate ions carried by the river varies little from season to season (Pelletier and
190 Lebel, 1979). On a yearly basis, between 15-20 % of the outflow of dissolved inorganic
191 carbon from the St. Lawrence River into its estuary originates from the system's
192 tributaries (e.g., Ottawa River, Mascouche River) while 80-85 % is from the Great Lakes
193 (Hélie et al., 2002). The St. Lawrence Estuary (SLE) begins at the landward limit of the
194 salt water intrusion near Île d'Orléans (~5 km downstream of Québec City) and
195 stretches 400 km seaward to Pointe-des-Monts where it widens into the Gulf of St.
196 Lawrence (GSL) (El-Sabh and Silverberg, 1990), a semi-enclosed sea with an area of
197 approximately 240,000 km² (Dufour and Ouellet, 2007) connected to the Atlantic
198 Ocean through Cabot Strait and the Strait of Belle Isle (Coote and Yeats, 1979).

Deleted: ~

199
200 Traditionally, the SLE is divided into two segments based on its bathymetry and
201 hydrographical features (Ingram and El-Sabh, 1990). The Upper St. Lawrence Estuary
202 (USLE), from Île d'Orléans, where the estuarine circulation begins, to Tadoussac, near
203 the mouth of the Saguenay Fjord, covers an area of 3,470 km². It is relatively narrow (2
204 to 24 km wide) and mostly shallow (depths less than 30 m; d'Anglejan, 1990), and
205 features an uneven, fairly complex bottom topography characterized by several
206 disconnected channels and troughs separated by ridges and islands (El-Sabh and
207 Murty, 1990). Topographically modified flows give rise to very large tidal ranges and
208 currents (up to 10 m and 3 m s⁻¹, respectively; Mertz and Gratton, 1990). In this tidally
209 energetic region, wind mixing is one to two orders of magnitude smaller than tidal
210 mixing (Painchaud et al., 1995). Owing to the resuspension of bottom sediments (tide,
211 wind or wave generated) and the net non-tidal estuarine circulation (d'Anglejan and
212 Smith, 1973), a well-developed turbidity maximum stretches between Île d'Orléans
213 and Île-aux-Coudres (Painchaud and Therriault, 1989) where suspended particulate

Deleted: , just downstream of Québec City,

Deleted: motions

Deleted: ~

218 matter concentrations vary from 10 to more than 200 mg l⁻¹ (Silverberg and Sundby,
219 1979). The sources of particulate organic matter (POM) in the estuary are still debated
220 (Gearing and Pocklington, 1990). Carbon isotope studies indicate that less than half of
221 the POM is derived from terrestrial sources (Pocklington and Leonard, 1979) and is
222 quite refractory to biodegradation (Lucotte et al., 1991), whereas the major contributor
223 to POM is believed to be “fresh” organic matter, i.e., living or recently living material,
224 of river-borne origin (Tan and Strain, 1983; Hélie and Hillaire-Marcel, 2006). During the
225 spring freshet in April-May, when freshwater discharge delivers 40 % of the annual
226 solid inputs to the estuary, the input of terrigenous POM is equivalent to the average
227 POM kept in suspension in the turbidity maximum (Lucotte, 1989).

Deleted: -

228
229 The Lower St. Lawrence Estuary (LSLE) is fairly unique in that its character is more
230 oceanic than most estuaries due to its grand size in all three dimensions and
231 unimpeded connection with Labrador and Slope waters from the Atlantic Ocean (El-
232 Sabh and Silverberg, 1990). Relative to the USLE, the LSLE is much larger (9,350 km²;
233 d'Anglejan, 1990), wider (30 to 50 km) and deeper (~300 m), and displays a smoother,
234 less variable bottom topography. Tidal currents are weaker (on the order of 30 cm s⁻¹
235 or less; Mertz and Gratton, 1990) and, under these less turbulent conditions, the Lower
236 Estuary is the major sink of continental inputs to the St. Lawrence system. Most (~75 %)
237 of the terrigenous POM carried by the St. Lawrence River is deposited on the LSLE floor
238 (Lucotte et al., 1991). The dominant bathymetric feature of the LSLE is the Laurentian
239 Channel (or Trough), a deep, central, U-shaped glaciated valley that extends 1,240 km
240 from the eastern Canadian continental shelf break through the GSL and into the LSLE
241 (d'Anglejan, 1990). The termination (head) of the Laurentian Channel at an abrupt and
242 shallow sill near Tadoussac marks the region of transition between the Upper and
243 Lower Estuary and is an area of complex tidal phenomena (Gratton et al., 1988). Due
244 to rapid shoaling, tidal movements (e.g., internal tides and strong flows over the steep
245 sill) locally generate significant mixing of surface freshwater with cold, nutrient-rich
246 waters from the intermediate and deep layers of the Gulf, resulting in a fertile surface
247 layer that flows continuously seaward (Coote and Yeats, 1979; Saucier and Chassé,
248 2000) and sustains important feeding habitats for several large marine mammals
249 (Dufour and Ouellet, 2007). The Lower Estuary's seaward outflow, together with the
250 Gaspé Current, a rapidly moving coastal jet, are a major input of nutrients and
251 zooplankton to the near-surface waters of the GSL (Coote and Yeats, 1979; Plourde

Deleted: -

Deleted: , at the mouth of the Saguenay Fjord,

Deleted: , including

Deleted: ,

Deleted: near-surface

Deleted: s

Deleted: deeper saline waters

Deleted: an important feeding habitat for several large marine mammals (Dufour and Ouellet, 2007) as well as

Deleted: nutrient-rich

Deleted: continuously through the LSLE

265 and Runge, 1993). Mesoscale features such as coastal jets, internal Kelvin waves,
266 baroclinic eddies and unstable waves are all possible due to strong Coriolis effects
267 (Ingram and El-Sabh, 1990).

268

269 The Lower St. Lawrence Estuary is one of the most laterally stratified estuaries in
270 the world (Larouche et al., 1987), and is also strongly vertically stratified. During
271 summertime, the SLE can be described as a three-layer system on the basis of its
272 thermal stratification (Gratton et al., 1988). Each spring, a new surface layer flow is
273 initiated by the freshwater runoff from the St. Lawrence River, Saguenay Fjord and
274 rivers on the north shore of the estuary (Dufour and Ouellet, 2007; see Fig. 1).
275 Discharge from the St. Lawrence River (mean annual discharge of $10,000 \text{ m}^3 \text{ s}^{-1}$,
276 peaking at $15,000 \text{ m}^3 \text{ s}^{-1}$ during the spring freshet; Painchaud and Therriault, 1989)
277 provides about 80 % of the total freshwater input to the estuary (Ingram and El-Sabh,
278 1990), whereas the combined runoff from the Saguenay and Manicouagan Rivers
279 accounts for most of the remainder (Tee, 1990). The warm and relatively fresh surface
280 layer (0 to 30 m) overlies the cold intermediate layer or CIL (30–150 m deep; $S_p = 32.0$
281 to 32.6) that is formed by advection of the Gulf's wintertime surface mixed layer
282 (Galbraith, 2006). Below the CIL, a warmer (2 to 6 °C) and saltier ($S_p = 33$ to 35) bottom
283 layer (>150 m deep), originating from the mixing of western-central Atlantic and
284 Labrador shelf waters that intrude at depth primarily through Cabot Strait, flows
285 sluggishly landward ($\sim 0.5 \text{ cm s}^{-1}$; Bugden, 1988) toward the head region of the
286 Laurentian Channel (Saucier et al., 2003; Gilbert et al., 2005).

287

288 2.2. Water-column sampling and analytical procedures

289

290 Water samples were collected aboard the RV Coriolis II during ten research
291 cruises within the St. Lawrence Estuary and Gulf in the ice-free spring or summer season
292 between 2003 and 2016. Water sampling was conducted mainly along the central axis
293 of the St. Lawrence Estuary and the Laurentian Channel. The sampling locations are
294 shown in Fig. 2. Samples were taken from discrete depths throughout the water
295 column, typically at 3 m, 20 m, 50 m, 70 m, 100 m and at 50m intervals to the bottom
296 (or within 10 m of the bottom). A comprehensive dataset was compiled from field or
297 laboratory measurements of the following physical–chemical properties: temperature
298 (T), practical salinity (S_p), pH_{NBS} and/or pH_{T} , total alkalinity (TALK), dissolved inorganic

Deleted: .

Deleted: -

Deleted: -

Deleted: r

Deleted: the

Deleted: from the GSL

Deleted: -

Deleted: on

Deleted: The sampling locations are shown in Fig. 2. Samples were taken at ~3m depth and throughout the water column, along the central axis of the estuary and Laurentian Channel, and in the freshwaters of the St. Lawrence River near Québec City, to obtain freshwater and seawater end-member values

Deleted: .

Deleted: describing the inorganic carbon chemistry in surface mixed layer waters

316 carbon (DIC), soluble reactive phosphate (SRP), and dissolved silicate (DSi), nitrate
317 (NO_3) and oxygen (DO).

318

319 T and S_P were determined *in situ* using the conductivity-temperature-depth
320 (CTD) probe (SeaBird SBE 911) mounted on the sampling rosette. The temperature
321 probe was calibrated by the manufacturer, whereas the conductivity sensor was
322 calibrated by the manufacturer and recalibrated using discrete salinity samples
323 collected throughout the water column and analyzed on a Guildline Autosal 8400
324 salinometer calibrated with IAPSO standard seawater. Water samples destined for pH
325 and TAlk measurements were transferred directly from the 12L Niskin bottles mounted
326 on the CTD-rosette system to, respectively, 125mL plastic bottles without headspace
327 and 250mL glass bottles as soon as the rosette was secured onboard. In the latter case,
328 a few crystals of HgCl_2 were added before the bottle was sealed with a ground-glass
329 stopper and Apiezon® Type-M high-vacuum grease.

330

331 pH was determined onboard at 25 °C, potentiometrically on the NBS/NIST scale
332 (infinite dilution convention, pH_{NBS}) for low salinity waters ($S_P < 5$) and
333 potentiometrically and/or colorimetrically on the total hydrogen ion concentration
334 scale (constant ionic medium convention, pH_T) for higher salinity waters.
335 Potentiometric pH measurements were carried out using a Radiometer Analytical®
336 GK2401C combination glass electrode connected to a Radiometer Analytical® PHM84
337 pH/millivolt-meter. Prior to each measurement, the electrode was calibrated against
338 three NIST-traceable buffer solutions: pH-4.00, pH-7.00 and pH-10.00 at 25°C. The
339 electrode response to these buffers was then least-squares fitted to obtain the
340 Nernstian slope. For $S_P > 5$, pH measurements were converted to the pH_T scale using
341 TRIS buffer solutions prepared at $S_P = 5, 15, 25, \text{ or } 35$ for which the pH_T was assigned
342 at 25°C (Millero, 1986). Colorimetric pH measurements were carried out using a
343 Hewlett-Packard UV-Visible diode array spectrophotometer (HP-8453A) and a 5cm
344 quartz cell after thermal equilibration of the plastic sampling bottles in a constant
345 temperature bath at $25.0 \pm 0.1^\circ\text{C}$. Phenol red (Robert-Baldo et al., 1985) and *m*-cresol
346 purple (Clayton and Byrne, 1993) were used as color indicators. The pH_T of the water
347 samples and buffer solutions were calculated according to the equation of Byrne
348 (1987). The reproducibility of the pH measurements was typically better than ± 0.003 .

349

350 TAlk was measured at McGill University using an automated Radiometer
351 (TitraLab865®) potentiometric titrator and a Red Rod® combination pH electrode
352 (pHC2001). The dilute HCl titrant was calibrated prior, during, and after each titration
353 session using certified reference materials provided by Andrew Dickson (Scripps
354 Institute of Oceanography). Raw titration data were processed with a proprietary
355 algorithm specifically designed for shallow end-point detection. The reproducibility of
356 the method was better than 0.5 %.

357

358 Direct DIC measurements were carried out during an additional cruise in 2014
359 using a Scitech Apollo DIC analyzer. After being thermostated at 25 °C, 1-1.5 mL of the
360 sample was injected into the instrument's reactor where it was acidified with 10 %
361 H₃PO₄ and the evolved CO₂ carried by a stream of pure nitrogen to a LICOR infrared
362 analyzer. A calibration curve was constructed using gravimetrically-prepared Na₂CO₃
363 solutions, and the accuracy of the measurements was verified using certified reference
364 material solutions provided by Andrew Dickson (Scripps Institute of Oceanography).
365 The reproducibility of the measurements was typically on the order of 0.2 %. Results of
366 the direct DIC measurements were used to assess the contribution of organic alkalinity
367 to the total alkalinity in the Upper Estuary, as discussed in Section 2.3.2.

368

369 DO concentrations were determined by Winkler titration (Grasshoff et al., 1999)
370 on distinct water samples recovered directly from the Niskin bottles. The relative
371 standard deviation, based on replicate analyses of samples recovered from the same
372 Niskin bottle, was better than 1 %. These measurements further served to calibrate the
373 SBE-43 oxygen probe mounted on the rosette. For the determination of nutrient
374 concentrations, aliquots of the water samples taken from the Niskin bottles were
375 syringe filtered through a 0.45µm Millipore polycarbonate (MA) filter. DSi was
376 measured onboard on the same day of sampling using the method described in
377 Grasshoff et al. (1999). Water samples destined for NO₃ and SRP measurements were
378 transferred, respectively, into acid-washed 15ml polyethylene and borosilicate tubes,
379 quickly frozen and stored at -20 °C. Their concentrations were determined using
380 standard colorimetric methods adapted from Grasshoff et al. (1999) with a SEAL
381 Autoanalyzer III at the Institut des Sciences de la Mer de Rimouski. The analytical
382 detection limit was 0.04 µM for NO₃, 0.05 µM for SRP and 0.1 µM for DSi. Based on

Formatted: Indent: First line: 0.5"

383 replicate analyses of the standards, the reproducibility of these measurements was
384 typically 1 %.

385

386 The *in situ* pressure and density of the samples were calculated from the
387 Thermodynamic Equation of Seawater - 2010 (TEOS-10) using the Gibbs Seawater
388 (GSW) Oceanographic Toolbox (MATLAB-version 3.05; McDougall and Barker, 2011).
389 All field measurements reported in $\mu\text{mol L}^{-1}$ were converted to $\mu\text{mol kg}^{-1}$ using the *in*
390 *situ* density data.

391

392 2.3. Calculation of aqueous pCO_2

393

394 2.3.1. pCO_2 in mixed-layer waters

395

396 Aqueous pCO_2 ($\text{pCO}_2(\text{water})$) is defined as the partial pressure of carbon
397 dioxide in wet (100 % water-saturated) air that is in equilibrium with the water sample.

398 *Because direct pCO_2 measurements were not available from the RV Coriolis II cruises,*

399 $\text{pCO}_2(\text{water})$ (μatm) *and* DIC ($\mu\text{mol kg}^{-1}$) were calculated from the measured pH (total
400 or NBS scale) and TALK ($\mu\text{mol kg}^{-1}$), at *in situ* temperature ($^{\circ}\text{C}$), salinity (S_P) and pressure

401 (dbar), using the program CO2SYS (MATLAB-version 1.1; van Heuven et al., 2011) and
402 the carbonic acid dissociation constants (K_1 , K_2) of Cai and Wang (1998) for estuarine

403 waters. Wherever data were available, the contributions to TALK from phosphate and
404 silicate were included *in the calculations*. Although the K_1 and K_2 formulations from

405 Lueker et al. (2000) are recommended for best practices by Dickson et al. (2007), they
406 are not suitable for the low-salinity conditions found in estuaries ($S_P < 19$) (Orr et al.,
407 2015). The revised equations for K_1 and K_2 from Cai and Wang (1998) are applicable

408 over a larger range of salinities (0 to 40) and, thus, were used to examine the carbonate
409 system in the estuarine waters of our study area.

410

411 This study focuses on the CO_2 dynamics *in* near-surface waters. To obtain
412 individual data points of surface-water pCO_2 at each sampling location, the pCO_2 data

413 in the surface mixed layer (SML) were averaged. The SML is the site of active air-sea
414 interaction where heat and gases are exchanged directly with the atmosphere and
415 within which physical (temperature, salinity, density) and chemical (dissolved gases)

416 properties are vertically homogeneous due to turbulent mixing (Sprintall and Tomczak,

Deleted: -

Deleted: -

Deleted: surface

Deleted:

Formatted: Not Superscript/ Subscript

Formatted: Font:Italic

Deleted: Values of

Formatted: Not Superscript/ Subscript

Deleted: and total dissolved inorganic carbon, or

Deleted: -

Deleted: ,

Deleted: -

Deleted: ,

Deleted: and

Deleted: ,

Deleted: inorganic carbon

Deleted: of

Deleted: (water)

432 1992). The lower limit to air-sea interaction, i.e., the mixed layer depth (MLD), is
433 demarcated by a pycnocline, a sharp density gradient that generally coincides with
434 both a temperature (thermocline) and salinity (halocline) gradient. Here, we determine
435 the thickness of the SML using a density-based criterion which defines the MLD as the
436 depth at which a threshold difference of 0.03 kg m^{-3} from the sea surface occurs (de
437 Boyer Montégut et al., 2004). In the following sections, surface-water pCO_2 will be
438 taken to mean the SML-averaged pCO_2 .

439

440 2.3.2. Sources of error in pCO_2 calculation

441

442 In this study, pH/Talk was used as the input combination to study the
443 consistency between calculations of pCO_2 using different sets of carbonic acid
444 dissociation constants. The importance of using appropriate formulations of K_1 and K_2
445 in estuarine waters is shown by the discrepancies in the calculated pCO_2 values (pCO_2
446 @ 15°C) at low salinities (Fig. 3). The percent difference between values calculated
447 using the dissociation constants of Cai and Wang (1998) and those calculated using
448 the best-practices constants of Lueker et al. (2000) was on average 3.07%. At $S_p < 19$,
449 differences between the calculated pCO_2 values were as large as 18.0% (average
450 difference of 6.88%), whereas, at $S_p > 19$, the calculated values were in better
451 agreement (only ~1.48% difference). The K_1 and K_2 formulations of Millero (2010), the
452 most recent set of constants proposed for estuarine waters ($S_p = 1$ to 50), yielded pCO_2
453 values that differed substantially from those derived using the constants of Cai and
454 Wang (1998) at $S_p < 19$, with the largest divergence reaching 34.4% (average
455 difference of 13.6%). At $S_p = 0$, the pCO_2 values calculated using the constants of Cai
456 and Wang (1998) compared very well with those given by the Millero (1979) constants
457 for freshwater (difference of only ~0.08%), whereas the pCO_2 values calculated using
458 the constants of Millero (2010) showed very poor agreement with the freshwater results
459 (differing by ~34.3%). These discrepancies highlight the need for new or revised
460 measurements of the carbonic acid dissociation constants under estuarine conditions
461 (in brackish waters) especially at $S_p < 5$. Studies which use the best-practices
462 formulations of K_1 and K_2 to calculate estuarine pCO_2 may underestimate CO_2
463 emissions at low salinities, whereas those that implement the Millero (2010)
464 formulations may produce overestimates.

465

Deleted: the

Deleted: , in which the

Deleted: is defined

Deleted: -

Deleted: calculated values

Deleted: of pCO_2 (pH/Talk)

Deleted: pCO_2 values calculated from

Deleted: from

Deleted: 2.12

Deleted: Calculations differed by 1.13-

Deleted: 5

Deleted: at low salinities ($S_p < 19$)

Deleted: pCO_2

Deleted: much closer

Deleted: 9

Deleted: i.e.,

Deleted: alternative

Deleted: that differ

Deleted: d

Deleted: of

Deleted: 5

Deleted: 7

Deleted: from

Deleted: values

Deleted: calculated from

491 Another potential source of error in the calculation of pCO₂ (pH/Talk) in low-
492 salinity estuarine waters is the contribution of dissolved organic compounds to the total
493 alkalinity. The contributions of borate, phosphate and silicate species are taken into
494 consideration in CO2SYS, whereas the magnitude of organic alkalinity (Org-Alk, or
495 excess alkalinity) is usually assumed to be small or negligible, and is simply ignored
496 when using TALK to calculate pCO₂ in open ocean waters. In riverine and coastal waters,
497 however, the contribution of organic species to the TALK can be significant (Yang et al.,
498 2015). Rivers draining organic-rich soils and non-carbonate rocks have low DIC
499 concentrations (a few hundred μmol L⁻¹) that are often exceeded by dissolved organic
500 carbon (DOC) concentrations (Abril et al., 2015). As discussed by Hunt et al. (2011), a
501 significant contribution of Org-Alk (the organic acid anions in DOC) leads to an
502 overestimation of calculated pCO₂ using any algorithm that accounts only for the
503 contributions of inorganic species to TALK. A comparison of the calculated TALK
504 (DIC/pH) and the measured TALK from the 2014 cruise reveals that Org-Alk is on the
505 order of -20 μmol kg⁻¹ for the St. Lawrence River end-member, whereas it is as high as
506 -120 μmol kg⁻¹ for the Saguenay River end-member (A. Mucci, pers. comm.). Given that
507 TALK exceeds ~1000 μmol kg⁻¹ throughout our study area and the Saguenay River
508 contribution to the surface waters of the SLE is limited (at most ~6 % at the head of the
509 Lower Estuary; Mucci et al., in revision), consideration of the Org-Alk in the calculation
510 of pCO₂ (pH/Talk) yielded values that were at most 1.9 % different from those
511 uncorrected for Org-Alk. Bearing in mind the uncertainties in the K₁ and K₂
512 formulations as well as the analytical uncertainties, the influence of Org-Alk on the
513 calculated pCO₂ (pH/Talk) did not represent a significant source of error.

514

515 2.4. Temperature normalization of pCO₂

516

517 The effect of temperature on aqueous pCO₂ is primarily the manifestation of
518 changes in the solubility of CO₂ gas in water (Takahashi et al., 1993). The temperature
519 dependence of pCO₂ in seawater, i.e., $\partial \ln(p\text{CO}_2) / \partial T = 0.0423 \text{ } ^\circ\text{C}^{-1}$, was determined
520 experimentally by Takahashi et al. (1993) on a single North Atlantic surface water
521 sample with S_P = 35.380 under isochemical conditions. As this oft-used approximation
522 for thermally induced changes in pCO₂ was derived from direct measurements in open
523 ocean waters, we use a different approach to remove the temperature effect on the
524 estuarine pCO₂ in our study area. The *in situ* pCO₂ were normalized to the average

Deleted: organic species

Deleted: While t

Deleted: by the program

Deleted: -

Deleted: program

Deleted: contributing

Deleted: (direct DIC measurements were carried out in 2014)

Deleted: -

Deleted: -

Deleted: -

Deleted: estuary

Deleted: submitted

Deleted: measurement

Deleted: calculation of

Deleted: -

Deleted: seawater

542 surface-water temperature ($pCO_2(SST)$, $SST = 7.82$ °C), using the temperature
 543 normalization method of Jiang et al. (2008) in which pCO_2 values are re-calculated from
 544 the TALK and DIC data at a common temperature. The results yielded a temperature
 545 coefficient of $\partial \ln(pCO_2) / \partial T = 0.0402$ °C⁻¹ ($R^2 = 0.99$), in excellent agreement with that
 546 of Takahashi et al. (1993). The pCO_2 changes due to temperature deviations from SST
 547 ($\Delta pCO_2(temp)$) were calculated as:

$$549 \Delta pCO_2(temp) = pCO_2(obs) - pCO_2(SST) \quad (1)$$

551 where $pCO_2(obs)$ is the *in situ* pCO_2 and $pCO_2(SST)$ is the temperature-normalized
 552 pCO_2 . Since changes in pCO_2 at a common temperature primarily reflect changes in
 553 DIC, the spatial variations in $pCO_2(SST)$ can be attributed to the combined influences
 554 of non-thermal processes that affect DIC (water mass mixing, biological activity).
 555 Theoretically, $pCO_2(SST)$ can be further partitioned into the pCO_2 change due to
 556 biology and that due to mixing through an analysis of the water mass structure, e.g., an
 557 optimum multiparameter (OMP) water mass analysis. Results from its application will
 558 be presented in a subsequent study.

560 2.5. Air-sea CO₂ flux estimation

562 Air-sea CO₂ gas exchange (F , mmol C m⁻² d⁻¹) at each sampling location was
 563 estimated as follows:

$$565 F = k \cdot K_0 \cdot (pCO_2(water) - pCO_2(air)) \quad (2)$$

567 where k (cm h⁻¹) is the gas transfer velocity of CO₂, K_0 (mol kg⁻¹ atm⁻¹) is the solubility
 568 coefficient of CO₂ at *in situ* surface-water temperature and salinity (Weiss, 1974), and
 569 $pCO_2(water)$ and $pCO_2(air)$ (µatm) are the partial pressures of CO₂ in the water and the
 570 air, respectively. The difference between $pCO_2(water)$ and $pCO_2(air)$ (ΔpCO_2)
 571 determines the direction of gas exchange across the air-sea interface. Positive values
 572 of F indicate CO₂ release by the surface water, whereas negative values indicate CO₂
 573 uptake. Conversion factors were applied to express the final F with the aforementioned
 574 units.

Deleted: SST =

Deleted: 4

Deleted: -

Deleted: the mean SST

Deleted: $\Delta pCO_2(thermal)$

Deleted: $pCO_2(in-situ)$

Deleted: $pCO_2(temp-norm)$

Deleted: $\Delta pCO_2(thermal)$ is the pCO_2 change due to temperature effects,

Deleted: (in-situ)

Deleted: $pCO_2(temp-norm)$

Deleted: constant

Deleted: temperature-normalized pCO_2 were

Deleted:

Deleted: , i.e.,

Deleted: and

Deleted: $pCO_2(temp-norm)$

Deleted: pCO_2

Deleted: -

Deleted: -

Deleted: $pCO_2(water)$

Deleted: $pCO_2(air)$

Deleted: -

Deleted: -

Deleted: -

Formatted: Not Superscript/ Subscript

Formatted: Not Superscript/ Subscript

Formatted: Not Superscript/ Subscript

Formatted: Not Superscript/ Subscript

Deleted: of CO₂

Deleted: by the surface water

603 Atmospheric $p\text{CO}_2$ ($p\text{CO}_2(\text{air})$) was calculated using the monthly averages of the
604 measured mole fraction of CO_2 in dry air ($x\text{CO}_2$, at the greenhouse gas observational
605 station in Fraserdale, Ontario) obtained from the Climate Research Division at
606 Environment and Climate Change Canada. The mean $p\text{CO}_2(\text{air})$ in the sampling month
607 was computed using the relationship (Takahashi et al., 2002):

$$609 \quad p\text{CO}_2(\text{air}) = x\text{CO}_2 \cdot (P_b - P_w) \quad (3)$$

610
611 where $x\text{CO}_2$ is in ppm, P_b (atm) is the atmospheric (or barometric) pressure at the sea
612 surface, and P_w (atm) is the equilibrium (or saturation) water vapor pressure at *in situ*
613 surface-water temperature and salinity (Weiss and Price, 1980). One-month averaged
614 barometric pressures were calculated using the hourly station pressure data from
615 Environment Canada at the following weather observing stations: Québec/Jean
616 Lesage International Airport (Upper Estuary), Mont-Joli Airport (Lower Estuary), and
617 Gaspé Airport (Gulf of St. Lawrence). The P_b at station elevation was converted to mean
618 sea level pressure using the formula of Tim Brice and Todd Hall (NOAA's National
619 Weather Service, http://www.weather.gov/epz/wxcalc_stationpressure).

620
621 The formulation of the gas transfer velocity, k , is the largest source of error in the
622 computation of air-sea CO_2 fluxes (Borges et al., 2004a,b). Properly constraining values
623 of k in estuaries is problematic (Raymond and Cole, 2001) due to their hydrodynamic
624 and geomorphologic complexity (Abril et al., 2000). Gas transfer is thought to be
625 regulated by turbulence at the air-water interface (Wanninkhof, 1992). Wind stress
626 plays a key role in the generation of turbulence at the ocean surface through the
627 transfer of momentum to waves and currents (Ho et al., 2011), whereas, in estuarine
628 environments and especially macrotidal estuaries, surface turbulence can be created
629 by interactions of wind forcing, tidal currents and boundary friction (Zappa et al., 2003,
630 Borges et al., 2004a,b; Zappa et al., 2007) and, in turbid estuaries, attenuated by
631 suspended material (Abril et al., 2009). The turbulence generated from bottom stress
632 varies with water depth and tidal velocity (Raymond et al., 2000), and is important only
633 in shallower estuaries with high current velocities (Cercio, 1989). Raymond and Cole
634 (2001) have shown that wind stress controls turbulence at the air-water interface for all
635 systems with depths greater than 10 meters (at depths < 10 m, either wind or bottom
636 stress may dominate).

Formatted: Not Superscript/ Subscript

Formatted: Not Superscript/ Subscript

Deleted: $p\text{CO}_2(\text{air})$

Deleted: speeds

639
640
641
642
643
644
645
646
647
648
649
650
651
652
653
654
655
656
657
658
659
660
661
662
663
664
665
666
667
668
669
670
671
672

Several different predictive relationships between wind speed and gas transfer velocity have been proposed based on laboratory and field studies. Here, we estimate the latter from short-term (or steady) wind speed measurements using the equations of Wanninkhof (1992) revised by Wanninkhof (2014) and Raymond and Cole (2001):

k from Wanninkhof (2014), denoted as k_{W-14} :

$$k_{W-14} = 0.251 u^2 (Sc / 660)^{-0.5} \quad (4)$$

k from Raymond and Cole (2001), denoted as $k_{R\&C-01}$:

$$k_{R\&C-01} = 1.91 e^{0.35u} (Sc / 660)^{-0.5} \quad (5)$$

where u is the wind speed ($m\ s^{-1}$) and Sc is the Schmidt number ($Sc = \mu/D$, where μ is the kinematic viscosity of the water and D is the diffusion coefficient) for CO_2 gas in solution. The Schmidt number for CO_2 in seawater at $20\ ^\circ C$ is 660 and was adjusted to $Sc=600$ for freshwater. Hourly wind speed data were obtained from Environment Canada at the aforementioned weather observing stations, and averaged over the sampling month to obtain short-term wind speeds. The correction to a common Schmidt number was performed using the equations of Wanninkhof (1992) for the temperature dependence of Sc for CO_2 gas in seawater ($S_p=35$) and freshwater, respectively, and assuming that k is proportional to $Sc^{-0.5}$.

Because of increased turbulence, one would expect k values calculated from estuarine parameterizations to be higher than those predicted from oceanic parameterizations at equivalent wind speeds (Abril et al., 2000). Within the confines of the SLE, estimates of k using the Wanninkhof (2014) relationship ranged from 1.6 to 4.5 $cm\ h^{-1}$ whereas those calculated from Raymond and Cole (2001) were between 3.8 and 8.1 $cm\ h^{-1}$. Hence, we take the air-sea CO_2 flux values calculated with k_{W-14} to be the theoretical lower limit of gas exchange (F_{W-14}), whereas those computed from $k_{R\&C-01}$ represent the upper limit of gas exchange ($F_{R\&C-01}$).

In order to estimate the area-averaged CO_2 flux in the SLE, the estuary proper was divided into five segments, with each section containing at least one sampling location. Given that the Lower Estuary occupies ~75 % of the total estuarine surface

Deleted: gas transfer velocity

Deleted: -

Deleted: -

Deleted: -

Deleted: -

678 area, and encompasses a fairly wide range of pCO_2 values (standard deviation of 119
 679 μatm), the SLE was divided into longitudinal sections (Fig. 2) rather than segmented by
 680 salinity. The fluxes in each segment were normalized to the sectional surface area and
 681 then summed to obtain a spatially integrated air-sea CO_2 flux ($F_{area-avg}$) for the whole
 682 estuary, as follows (Jiang et al., 2008):

$$684 F_{area-avg} = \frac{\sum F_i S_i}{\sum S_i} \quad (6)$$

685 where F_i is the average of all the fluxes within segment i , and S_i is the surface area of
 686 segment i . Sectional surface areas were tabulated in MATLAB using the land mask of
 687 eastern Canada obtained from Fisheries and Oceans Canada. An area-averaged CO_2
 688 flux was obtained for both the upper and lower limits of gas exchange in the SLE. These
 689 two final estimates are assumed to bracket the real areal CO_2 flux.

692 2.6. Conceptual framework for the analysis of variations in biogenic gas 693 concentrations

694 A comparison of the distribution of biologically reactive dissolved gases, i.e.,
 695 CO_2 and O_2 , can provide useful information about the physical (thermal) and biological
 696 processes controlling their concentrations (Richey et al., 1988). Temperature-related
 697 gas solubility effects occur in the same direction for CO_2 and O_2 , whereas biological
 698 production and respiration affect CO_2 and O_2 in opposite directions. Following the
 699 approach of Carrillo et al. (2004), the saturation states (or % saturation) of pCO_2 and
 700 DO, with respect to the atmosphere, were compared in order to determine the relative
 701 importance of temperature effects (heating or cooling) and biological activity
 702 (photosynthesis or respiration) in the surface waters at each sampling location. The
 703 pCO_2 percent saturation ($pCO_2(\% sat)$) was calculated as follows:

$$706 pCO_2(\% sat) = (pCO_2(water) / pCO_2(air)) \cdot 100 \quad (7)$$

707 The DO percent saturation ($DO(\% sat)$) was calculated as:

$$710 DO(\% sat) = (DO / DO^*) \cdot 100 \quad (8)$$

711

Deleted: for
 Deleted: for air-sea gas exchange
 Deleted: in

Deleted: e.g

Deleted: changes

Deleted: %
 Formatted: Not Superscript/ Subscript
 Formatted: Not Superscript/ Subscript
 Deleted: % $pCO_{2(sat)}$
 Deleted: $pCO_{2(water)}$
 Deleted: $pCO_{2(air)}$ ²
 Deleted: %
 Formatted: Not Superscript/ Subscript
 Formatted: Not Superscript/ Subscript
 Deleted: % $DO_{(sat)}$

723 where DO^* is the equilibrium DO concentration ($\mu\text{mol kg}^{-1}$) at *in situ* surface-water
724 temperature and salinity (Benson and Krause, 1984). The relationship between DO(%
725 sat) and $p\text{CO}_2$ (% sat) is roughly analogous to that of the apparent oxygen utilization
726 (AOU) and excess DIC (eDIC) (Abril et al., 2000). The former is defined as the difference
727 between DO^* and DO, whereas the latter is defined as the difference between the
728 observed DIC and a theoretical DIC at atmospheric equilibrium.

Deleted: ~

729
730 According to the method of Carrillo et al. (2004), data points fall into one of four
731 quadrants on a graph of $DO(\% \text{ sat})$ versus $p\text{CO}_2(\% \text{ sat})$, with the origin at 100 %
732 saturation for both gases. Quadrant I (upper left; supersaturated DO, undersaturated
733 $p\text{CO}_2$) suggests net photosynthesis, Quadrant II (upper right; supersaturated DO and
734 $p\text{CO}_2$) indicates the effects of heating, Quadrant III (lower right; undersaturated DO,
735 supersaturated $p\text{CO}_2$) implies net respiration, and Quadrant IV (lower left;
736 undersaturated DO and $p\text{CO}_2$) represents the effects of cooling. Although general
737 patterns become apparent, we urge caution in the interpretation of these results as
738 significant limitations apply. Surface-water CO_2 and O_2 may be acted upon by other
739 forcings such as air-sea gas exchange. The net transfer of CO_2 and O_2 gases occurs
740 across the air-sea interface whenever their partial pressures in the SML differ from those
741 in the atmosphere. Because of their differential gas exchange rates (i.e., O_2 exchanges
742 ~19 times faster than CO_2 ; Peng et al., 1987), CO_2 and O_2 dynamics may be decoupled
743 in surface waters, causing an asymmetry in the observed $\text{CO}_2:\text{O}_2$ relationship (Carrillo
744 et al., 2004).

Deleted: %

Formatted: Not Superscript/ Subscript

Deleted: %

Formatted: Not Superscript/ Subscript

Formatted: Not Superscript/ Subscript

Formatted: Not Superscript/ Subscript

Deleted: the surface

Deleted: water

745 746 3. Results and discussion

747 748 3.1. Spatial variability of surface-water $p\text{CO}_2$

Deleted: variability

750 Data were compiled from all ten cruises to describe the inorganic carbon
751 chemistry in the mixed-layer waters of the St. Lawrence River, Upper Estuary, Lower
752 Estuary and Gulf (Table 1). Large spatial variations in surface-water $p\text{CO}_2$ were
753 observed with in the EGSL system, with values ranging from 139 to 765 μatm (452 ± 134
754 μatm) during the spring/summer sampling periods. Overall, the $p\text{CO}_2$ were higher in
755 the USLE ($571 \pm 72 \mu\text{atm}$) than in the LSLE ($394 \pm 119 \mu\text{atm}$) and GSL ($352 \pm 80 \mu\text{atm}$),
756 whereas the atmospheric $p\text{CO}_2$ showed less variability, ranging from 372 to 405 μatm ,

Deleted: SML

Deleted: variations

Deleted: 3

Deleted: 3

Deleted: T

Deleted: 7

Deleted: 4

Deleted: 2

771 during the sampling years. As shown in Fig. 4, the USLE was always a CO₂ source (i.e.,
772 surface-water pCO₂ were above atmospheric level) while the LSLE and GSL were
773 generally either a CO₂ sink or nearly neutral (i.e., surface-water pCO₂ were below or
774 close to atmospheric level).

775
776 Within the confines of the SLE, the surface-water pCO₂ generally decreased with
777 increasing distance from the head of the estuary (Île d'Orléans) and along the salinity
778 gradient (Fig. 4 and 5). The highest values of pCO₂ were observed near the landward
779 limit of the salt water intrusion in the SLE's upper reaches, in the vicinity of the Cap
780 Tourmente intertidal flats and marshes. This area (3 × 10⁶ m²) is located along the core
781 of the estuary's maximum turbidity zone (MTZ) (Lucotte and d'Anglejan, 1986). The
782 lowest surface-water pCO₂ were found downstream of the MTZ in the lower reaches of
783 the SLE near Pointe-des-Monts, where the channel widens into the gulf. Due to
784 favorable environmental conditions (nutrients, light, stratification), phytoplankton
785 blooms typically occur in late spring or early summer in the LSLE (Zakardjian et al.,
786 2000), with maximal biological production occurring in its downstream portion due to
787 the mixing of cold, nutrient-rich waters, upwelled at the head of the Laurentian
788 Channel, with warmer freshwaters flowing in from the north shore rivers (Savenkoff et
789 al., 1994). Seaward from the estuary-gulf boundary, the pCO₂ gradually increased from
790 207 to 478 µatm, coinciding with rising surface-water temperatures (T = 3.9 to 13.7 °C).

791
792 The spatial variability of surface-water pCO₂ due to temperature variations was
793 removed by normalizing the pCO₂ data to a common temperature (T = 7.82 °C). From
794 a comparison of the *in situ* and corresponding temperature-normalized pCO₂, spatial
795 variations in surface-water temperature lowered or raised the pCO₂ by -122 to 181
796 µatm within the EGSL system. The maximum (minimum) values of ΔpCO₂(temp),
797 expressed as a percent change, were 38 % (-14 %) in the USLE, 24 % (-20 %) in the
798 LSLE, and 29 % (-17 %) in the GSL. Temperature normalization, however, removed only
799 a small part of the overall spatial variability of surface-water pCO₂ (Fig. 6). Given that
800 the spread of the pCO₂(SST) data remained large (153–668 µatm; 447 ± 133 µatm),
801 most of the spatial variability in surface-water pCO₂ can be explained by non-thermal
802 physical and biological processes that affect DIC concentrations in the mixed layer.

803

804 3.2. Air-sea CO₂ flux and spatial integration

- Deleted: months
- Deleted: From
- Deleted: it can be seen that
- Deleted: (water)
- Formatted: Not Superscript/ Subscript
- Deleted: equilibrium
- Deleted: (water)
- Formatted: Not Superscript/ Subscript
- Deleted: equilibrium

- Deleted: a large increase in

- Deleted: A
- Deleted: shows that
- Deleted: changes in
- Deleted:
- Deleted: 70
- Deleted: (thermal)
- Deleted: 31
- Deleted: temperature-normalized pCO₂
- Deleted: 9
- Deleted: heterogeneity
- Deleted: (water mass mixing and/or biological activity)

824

825 Large spatial variations in the air-sea CO₂ flux were observed within the EGSL
 826 system during the spring/summer sampling months, with fluxes ranging from -21.9 to
 827 28.4 mmol m⁻² d⁻¹ (Fig. 7). Values of F were always positive in the USLE (2.0 to 28.4
 828 mmol m⁻² d⁻¹) and either negative or positive in the LSLE (-21.9 to 15.1 mmol m⁻² d⁻¹)
 829 and GSL (-8.4 to 3.6 mmol m⁻² d⁻¹). As expected, F_{R&C-01} (estuarine parameterization of
 830 k) were larger than F_{W-14} (oceanic parameterization of k) due to the inherently greater
 831 surface turbulence in estuarine systems. The average difference between CO₂ fluxes
 832 calculated using the two formulations of the gas transfer velocity (equations 4 and 5)
 833 was 71.7%. Details of the k and F values given by each parameterization of k are shown
 834 in Table 2. Irrespective of the parameterization, the calculated CO₂ fluxes were more
 835 positive in the USLE (9.2 ± 5.3 mmol m⁻² d⁻¹) than in the LSLE (0.8 ± 7.2 mmol m⁻² d⁻¹)
 836 and GSL (-1.2 ± 3.0 mmol m⁻² d⁻¹).

837
 838 The SLE was divided into five segments to obtain an area-averaged CO₂ flux for
 839 the whole estuary. The data used to calculate the F_{area-avg} are listed in Table 3. Overall,
 840 the SLE served as a weak source of CO₂ to the atmosphere at the time of sampling,
 841 with an area-averaged degassing flux of 0.98 to 2.02 mmol C m⁻² d⁻¹ (0.36 to 0.74 mol
 842 C m⁻² yr⁻¹) during the late spring and early summer. This efflux compares favorably with
 843 that of the Delaware Estuary (2.4 ± 4.8 mol C m⁻² yr⁻¹; Joesoef et al., 2015), another
 844 large estuarine system with a long water residence time, but is significantly lower than
 845 estimates in the marine-dominated Sapelo and Doboy Sound estuaries (10.5 to 10.7
 846 mol C m⁻² yr⁻¹; Jiang et al., 2008). From a compilation of 165 estuaries worldwide,
 847 almost all systems, with the exception of those in the Arctic (-1.1 mol C m⁻² yr⁻¹), serve
 848 as sources of CO₂ to the atmosphere (Chen et al., 2013). Chen et al. (2013) concluded
 849 that the world's upper estuaries (S_p < 2) are strong sources (39.0 ± 55.7 mol C m⁻² yr⁻¹),
 850 mid estuaries (2 < S_p < 25) are moderate sources (17.5 ± 34.2 mol C m⁻² yr⁻¹), and lower
 851 estuaries (S_p > 25) are weak sources (8.4 ± 14.3 mol C m⁻² yr⁻¹). Predictably, with its
 852 maritime region occupying almost three-fourths of the total surface area, the SLE
 853 behaves like an outer estuary with only small CO₂ evasion. The lack of temporal
 854 coverage of surface-water pCO₂ data, however, prevents us from reliably synthesizing
 855 an annual air-sea CO₂ flux.

856
 857 **3.3. Major drivers of estuarine pCO₂ variability**

Deleted: variability ...ariations inof...the air-sea CO₂ flux wereas...observed within the EGSL system during the spring/summer sampling periods...onths, with fluxes ranging from -21.9 to 28.4 mmol m⁻² d⁻¹ (Fig. 7). Values of F were always positive in the USLE (2.0 to 28.4 mmol m⁻² d⁻¹) and either negative or positive in the LSLE (-21.9 to 15.1 mmol m⁻² d⁻¹) and GSL (-8.4 to 3.6 mmol m⁻² d⁻¹). As expected, F_{R&C-01} (estuarine parameterization of k) were larger than F_{W-14} (oceanic parameterization of k) due to the inherently greater surface turbulence in estuarine systems. The average difference between CO₂ fluxes calculated from...sing the two formulations of the gas transfer velocity (equations 4 and 5) Wanninkhof (2014) and those from Raymond and Cole (2001)...was 71.75...%. Details of the k and F values given by each parameterization of the gas transfer velocity... are shown in Table 2. Irrespective of the parameterization, the calculated CO₂ fluxes were more positive in the USLE (9.2 ± 5.3 mmol m⁻² d⁻¹) than in the LSLE (0.8 ± 7.2...mmol m⁻² d⁻¹) and GSL (-1.21...± 3.0 mmol m⁻² d⁻¹)

Deleted: To obtain an area-averaged CO₂ flux for the whole estuar...y, t...e SLE was divided into five segments t... obtain an area-averaged CO₂ flux for the whole estuarywith each segment containing at least one sampling location... The data used to calculate the F_{area-avg}area-averaged CO₂ flux...are listed in Table 3. Overall, the SLE served as a weak source of CO₂ to the atmosphere at the time of sampling, with an area-averaged CO₂...degassing flux of 1.00...98 to 2.06...02 mmol C m⁻² d⁻¹ (0.37...36 to 0.75...74 mol C m⁻² yr⁻¹) during the late spring and early summer. This efflux compares favorably with that of the Delaware Estuary (2.4 ± 4.8 mol C m⁻² yr⁻¹; Joesoef et al., 2015), another large estuarine system with a long water residence time, but is significantly lower than estimates in the marine-dominated Sapelo and Doboy Sound estuaries (10.5 to 10.7 mol C m⁻² yr⁻¹; Jiang et al., 2008). From a compilation of 165 estuaries worldwide, almost all systems, with the exception of those in the Arctic (-1.1 mol C m⁻² yr⁻¹), serve as sources of CO₂ to the atmosphere (Chen et al., 2013). Chen et al. (2013) concluded that the world's upper estuaries (S_p < 2) are strong sources (39.0 ± 55.7 mol C m⁻² yr⁻¹), mid estuaries (2 < S_p < 25) are moderate sources (17.5 ± 34.2 mol C m⁻² yr⁻¹), and lower estuaries (S_p > 25) are weak sources (8.4 ± 14.3 mol C m⁻² yr⁻¹)

Deleted: controlling factors

962
963
964
965
966
967
968
969
970
971
972
973
974
975
976
977
978
979
980
981
982
983
984
985
986
987
988
989
990
991
992
993
994
995

The pCO₂ in the surface mixed layer is a function of its temperature (T), salinity (S_p), dissolved inorganic carbon (DIC) and total alkalinity (TAlk), as described by the following relationship (Takahashi et al., 1993):

$$dpCO_2 = (\partial pCO_2/\partial T)dT + (\partial pCO_2/\partial S_p)dS_p + (\partial pCO_2/\partial DIC)dDIC + (\partial pCO_2/\partial TAlk)dTAlk \quad (9)$$

Through changes in T, S_p, DIC and TAlk, variations of surface-water pCO₂ are mainly controlled by dynamic processes (water mass mixing), thermodynamic processes (temperature and salinity changes), air-sea gas exchange, and biological processes (photosynthesis, respiration) (Poisson et al., 1993). Among these, the effects of temperature and DIC, i.e., the addition or removal of DIC through biological activity and mixing processes, are generally the most important drivers of estuarine pCO₂ variability. In the absence of a significant source or sink of TAlk (e.g., calcium carbonate formation/dissolution, anaerobic organic matter decomposition), changes of DIC determine the buffer capacity (DIC/TAlk ratio) of the water. Whereas the physically and biologically induced changes of DIC/pCO₂ will be quantified in a future study, using a modified OMP water mass analysis, here, we evaluate the relative importance of thermal and biological processes in controlling the spatial distribution of pCO₂ in the St. Lawrence Estuary and Gulf.

To disentangle the biological and temperature effects on the spatial variability of pCO₂, the DO(% sat) were plotted against the pCO₂(% sat), with the origin at 100 % saturation for both gases. This simple approach uses the four possible combinations of pCO₂(% sat)/DO(% sat) as integrated measures of thermally and biologically induced changes. As shown in Fig. 8 (top), microbial respiration was the major driver of pCO₂ variability in the USLE, whereas photosynthesis and temperature were the dominant controls in the LSLE and GSL. We found similar results from a comparison of eDIC and AOU (Fig. 8, bottom). In the strongly stratified Lower Estuary, as well as near the estuary-gulf boundary, the biological drawdown of CO₂ counteracted the decrease in CO₂ gas solubility due to increasing temperature (Fig. 9). Its waters were mostly undersaturated with CO₂ with respect to the atmosphere (values of pCO₂ were below atmospheric level) despite a general trend of surface-water warming (T = 2.7 to 12.6

Deleted: in
Deleted: the
Deleted: inputs from interna
Deleted:
Deleted: (
Deleted:)
Deleted: external (physical mixing) sources
Deleted: variations in pCO ₂ due to water mass mi... [3]
Deleted: separated
Deleted: in a future study
Deleted: through a modified OMP water mass analysis,
Deleted: our study area
Deleted: variability
Deleted: %
Formatted: Not Superscript/ Subscript
Deleted: %
Formatted: Not Superscript/ Subscript
Formatted: Not Superscript/ Subscript
Formatted: Not Superscript/ Subscript
Deleted: %
Formatted: Not Superscript/ Subscript
Formatted: Not Superscript/ Subscript
Deleted: %
Formatted: Not Superscript/ Subscript
Formatted: Not Superscript/ Subscript
Deleted: From
Deleted: it can be seen that
Deleted: the
Deleted: effects of photosynthesis and temperat... [4]
Deleted:
Deleted: pCO ₂
Formatted: Not Superscript/ Subscript
Deleted: surpassed
Deleted: increasing effect of sea surface warming
Deleted: V
Deleted: surface-water
Deleted: mostly
Deleted:
Deleted: increases in temperature
Deleted: -0.32

1031 °C). This pattern is consistent with the finding that, in spring/summer, the increasing
1032 effect of warming on pCO₂ is counteracted by the photosynthetic utilization of CO₂,
1033 particularly in a strongly stratified shallow mixed layer (Takahashi et al., 1993). Whereas
1034 direct measurements of chlorophyll-a concentrations were not carried out during the
1035 research cruises, a fluorescence sensor was mounted on the CTD probe. As shown in
1036 Fig. 10, maximum fluorescence values, as well as high values of transmission (% light
1037 transmission approaching 100%), were observed in the eastern Lower Estuary and the
1038 western Gulf of St. Lawrence, where the system appears to shift from net heterotrophy
1039 to net autotrophy. Farther into the Gulf (near Anticosti Island), the temperature
1040 dependence of pCO₂ exerted a stronger influence, causing values of surface-water
1041 pCO₂ to increase concomitantly with temperature (Fig. 9).

Deleted: In
Deleted: of St. Lawrence
Deleted: major
Deleted: (207 to 478 μatm)
Deleted: (T = 3.9 to 13.7 °C)

1043 4. Conclusions

1044
1045 Because of its large physical dimensions and unimpeded connection to the
1046 Atlantic Ocean, the St. Lawrence Estuary encompasses both a river-dominated inner
1047 estuary, where physical mixing and abiotic processes dominate, and a marine-
1048 dominated outer estuary, where biological cycling and oceanic processes prevail. The
1049 physical and biogeochemical processes of these contrasting environments are
1050 reflected in the spatial distribution of surface-water pCO₂ (139-765 μatm). The shallow,
1051 partially mixed Upper Estuary, with a turbidity maximum controlled by tide- and wind-
1052 induced turbulence, was, during our sampling period, a net source of CO₂ to the
1053 atmosphere due to microbial respiration (low biological productivity), whereas the
1054 deep, stratified Lower Estuary, with its stable, summertime three-layer vertical
1055 structure, was generally a net sink of atmospheric CO₂ due to the enhanced biological
1056 drawdown of pCO₂ (light availability, nutrient supply, strong stratification).

Deleted: 1.00
Deleted: 2.06
Deleted: -
Deleted: -
Deleted: 0.37
Deleted: 0.75
Deleted: -
Deleted: -
Deleted: -
Deleted: -
Deleted: -
Deleted: -

1057
1058 Overall, the large subarctic St. Lawrence Estuary was a weak source of CO₂ to
1059 the atmosphere, with an area-averaged CO₂ degassing flux of 0.98 to 2.02 mmol C m⁻²
1060 d⁻¹ (0.36 to 0.74 mol C m⁻² yr⁻¹). This efflux is somewhat smaller than the numerically
1061 averaged CO₂ flux per unit area (2.19 mol C m⁻² yr⁻¹) reported from North American
1062 estuaries by Chen et al. (2013), highlighting their relatively small contribution (~12 %)
1063 to global estuarine CO₂ emissions. The pronounced shift in source/sink dynamics in
1064 the St. Lawrence Estuary, between its river-dominated (9.2 ± 5.3 mmol m⁻² d⁻¹) and

1082 marine-dominated ($0.8 \pm 7.2 \text{ mmol m}^{-2} \text{ d}^{-1}$) regions, is consistent with the conclusions
1083 of the comparative study carried out by Jiang et al. (2008) that **revealed** large
1084 differences in CO₂ degassing between riverine (inner) and maritime (outer) estuaries.
1085 Given the limited research on CO₂ dynamics in large estuaries and bay systems, which
1086 cover approximately one-half of the estuarine surface area on the U.S. east coast, as
1087 well as the large uncertainties in the **indirect measurement** of pCO₂ (carbonic acid
1088 dissociation constants, organic alkalinity contribution), current global-scale estimates
1089 of estuarine CO₂ degassing may be overestimated. To better constrain the role of large
1090 estuaries/bays in the **coastal ocean** carbon cycle, more extensive spatial and temporal
1091 coverage of **direct** pCO₂ measurements **across estuary types** is needed.

Deleted: 1

Deleted: -

Deleted: -

Deleted: showed

Deleted: calculation

Deleted: estuarine

1093 **Data availability**

1094 Data presented in this paper (Figures 4 and 8) are available upon request from one of the
1095 authors (alfonso.mucci@mcgill.ca).

1097 **Author contribution**

1098 A.D. and A.M. conceived the project. A.M. acquired and processed the data prior to 2016. A.D.
1099 conducted the data analysis and wrote the first draft of the paper whereas A.M. provided
1100 editorial and scientific recommendations.

1102 **Competing interests**

1103 The authors declare that they have no conflict of interest.

1105 **Acknowledgements**

1106 We wish to thank the Captains and crews of the RV *Coriolis II* for their unwavering help over
1107 the years. We also wish to acknowledge Gilles Desmeules and Michel Rousseau for their
1108 dedicated electronic and field sampling support as well as Constance Guignard for her help in
1109 cruise preparation and field data acquisition. Most of the data acquisition was carried out
1110 opportunistically on research cruises funded by grants to A.M. or Canadian colleagues by the
1111 Natural Sciences and Engineering Research Council of Canada (NSERC) whereas the work was
1112 funded by a Regroupement Stratégique grant from the Fonds Québécois de Recherche Nature
1113 et Technologies (FQRNT) to GEOTOP as well as NSERC Discovery and MEOPAR grants to A.M.
1114 A.D. wishes to thank the Department of Earth and Planetary Sciences at McGill for financial
1115 support in the form of scholarships and assistantships.

1117 **References**

1124
1125 Abril, G., Etcheber, H., Borges, A. V., and Frankignoulle, M.: Excess atmospheric carbon
1126 dioxide transported by rivers into the Scheldt estuary, *Cr. Acad. Sci. II A.*, 330, 761-768, 2000.
1127
1128 Abril, G., Commarieu, M. V., Sottolichio, A., Bretel, P., and Guerin, F.: Turbidity limits gas
1129 exchange in a large macrotidal estuary, [Estuar. Coast. Shelf Sci.](#), 83, 342-348, 2009.
1130
1131 Abril, G. et al.: Technical Note: Large overestimation of pCO₂ calculated from pH and alkalinity
1132 in acidic, organic-rich freshwaters, *Biogeosciences*, 12, 67-78, 2015.
1133
1134 Bauer, J. E., Cai, W. J., Raymond, P. A., Bianchi, T. S., Hopkinson, C. S., and Regnier, P. A.: The
1135 changing carbon cycle of the coastal ocean, *Nature*, 504, 61-70, 2013.
1136
1137 Benson, B. B. and Krause, D.: The concentration and isotopic fractionation of oxygen dissolved
1138 in freshwater and seawater in equilibrium with the atmosphere, *Limnol. Oceanogr.*, 29, 620-
1139 632, 1984.
1140
1141 Borges, A. V.: Do we have enough pieces of the jigsaw to integrate CO₂ fluxes in the coastal
1142 ocean?, *Estuaries*, 28, 3-27, 2005.
1143
1144 [Borges, A. V., and Abril, G.: Carbon dioxide and methane dynamics in estuaries, in: Wolanski,](#)
1145 [E. and McLusky, D. S. \(Eds.\), Treatise on Estuarine and Coastal Science, Academic Press,](#)
1146 [Waltham, 119-161, 2011.](#)
1147
1148 Borges, A. V., Delille, B., Schiettecatte, L. S., Gazeau, F., Abril, G., and Frankignoulle, M.: Gas
1149 transfer velocities of CO₂ in three European estuaries (Randers Fjord, Scheldt and Thames),
1150 *Limnol. Oceanogr.*, 49, 1630-1641, 2004a.
1151
1152 Borges, A. V., Vanderborght, J. P., Schiettecatte, L. S., Gazeau, F., Ferrón-Smith, S., Delille, B.,
1153 and Frankignoulle, M.: Variability of the gas transfer velocity of CO₂ in a macrotidal estuary (the
1154 Scheldt), *Estuaries*, 27, 593-603, 2004b.
1155
1156 Borges, A. V., Delille, B., and Frankignoulle, M.: Budgeting sinks and sources of CO₂ in the
1157 coastal ocean: Diversity of ecosystems counts, *Geophys. Res. Lett.*, 32, L14601,
1158 doi:10.1029/2005GL023053, 2005.
1159

Deleted: Estuar. Coast. Shelf S.

1161 Borges, A. V., Schiettecatte, L. S., Abril, G., Delille, B., and Gazeau, F.: Carbon dioxide in
1162 European coastal waters, Estuar. Coast. Shelf Sci., 70, 375-387, 2006.
1163
1164 Bugden, G. L.: Oceanographic conditions in the deeper waters of the Gulf of St. Lawrence in
1165 relation to local and oceanic forcing, NAFO SCR document 88/87, 1988.
1166
1167 Byrne, R. H.: Standardization of standard buffers by visible spectrometry, *Anal. Chem.*, 59,
1168 1479-1481, 1987.
1169
1170 Cai, W. J.: Estuarine and coastal ocean carbon paradox: CO₂ sinks or sites of terrestrial carbon
1171 incineration?, *Annual Review of Marine Science*, 3, 123-145, 2011.
1172
1173 Cai, W. J. and Wang, Y.: The chemistry, fluxes, and sources of carbon dioxide in the estuarine
1174 waters of the Satilla and Altamaha Rivers, Georgia, *Limnol. Oceanogr.*, 43, 657-668, 1998.
1175
1176 Carrillo, C. J., Smith, R. C., and Karl, D. M.: Processes regulating oxygen and carbon dioxide in
1177 surface waters west of the Antarctic Peninsula, *Mar. Chem.*, 84, 161-179, 2004.
1178
1179 Cerco, C. F.: Estimating estuarine reaeration rates, *J. Environ. Eng.-ASCE*, 115, 1066-1070,
1180 1989.
1181
1182 Chen, C. T. A. and Borges, A. V.: Reconciling opposing views on carbon cycling in the coastal
1183 ocean: continental shelves as sinks and near-shore ecosystems as sources of atmospheric CO₂,
1184 *Deep-Sea Res. Pt. II*, 56, 578-590, 2009.
1185
1186 Chen, C. T. A., Huang, T. H., Fu, Y. H., Bai, Y., and He, X.: Strong sources of CO₂ in upper
1187 estuaries become sinks of CO₂ in large river plumes, *Current Opinion in Environmental*
1188 *Sustainability*, 4, 179-185, 2012.
1189
1190 Chen, C. T. A., Huang, T. H., Chen, Y. C., Bai, Y., He, X., and Kang, Y.: Air-sea exchanges of CO₂
1191 in the world's coastal seas, *Biogeosciences*, 10, 6509-6544, 2013.
1192
1193 Clayton, T. D. and Byrne, R. H.: Spectrophotometric seawater pH measurements: total
1194 hydrogen ion concentration scale calibration of m-cresol purple and at-sea results, *Deep-Sea*
1195 *Res. Pt. I*, 40, 2115-2129, 1993.
1196

Deleted: Estuar. Coast. Shelf S.

1198 Cloern, J. E.: Our evolving conceptual model of the coastal eutrophication problem, *Mar. Ecol.-*
1199 *Prog. Ser.*, 210, 223-253, 2001.

1200

1201 Coote, A. R. and Yeats, P. A.: Distribution of nutrients in the Gulf of St. Lawrence, *J. Fish. Res.*
1202 *Board Can.*, 36, 122-131, 1979.

1203

1204 [Cotovicz Jr., L. C., Knoppers, B. A., Brandini, N., Costa Santos, S. J., and Abril, G.: A strong CO₂](#)
1205 [sink enhanced by eutrophication in a tropical coastal embayment \(Guanabara Bay, Rio de](#)
1206 [Janeiro, Brazil\), *Biogeosciences*, 12, 6125-6146, 2015.](#)

1207

1208 Cyr, F., Bourgault, D., Galbraith, P. S., and Gosselin, M.: Turbulent nitrate fluxes in the Lower St.
1209 Lawrence Estuary, Canada, *J. Geophys. Res.-Oceans*, 120, 2308-2330, 2015.

1210

1211 d'Anglejan, B.: Recent sediments and sediment transport processes in the St. Lawrence
1212 Estuary, in: El-Sabh, M. I. and Silverberg, N. (Eds.), *Oceanography of a Large-scale Estuarine*
1213 *System*, Springer-Verlag, New York, 109-129, 1990.

1214

1215 d'Anglejan, B. F. and Smith, E. C.: Distribution, transport, and composition of suspended
1216 matter in the St. Lawrence estuary, *Can. J. Earth Sci.*, 10, 1380-1396, 1973.

1217

1218 de Boyer Montégut, C., Madec, G., Fischer, A. S., Lazar, A., and Iudicone, D.: Mixed layer depth
1219 over the global ocean: An examination of profile data and a profile-based climatology, *J.*
1220 *Geophys. Res.*, 109, C12003, doi:10.1029/2004JC002378, 2004.

1221

1222 Dickson, A. G. and Goyet, C. (Eds.): *Handbook of Methods for the Analysis of the Various*
1223 *Parameters of the Carbon Dioxide System in Sea Water (Version 2)*, U.S. Department of Energy,
1224 ORNL/CDIAC-74, 1994.

1225

1226 Dickson, A. G., Sabine, C. L., and Christian, J. R. (Eds.): *Guide to Best Practices for Ocean CO₂*
1227 *Measurements*, PICES Special Publication 3, 191 pp., 2007.

1228

1229 Dufour, R. and Ouellet, P.: Estuary and Gulf of St. Lawrence marine ecosystem overview and
1230 assessment report, *Can. Tech. Rep. Fish. Aquat. Sci.*, 2744E, 112 pp., 2007.

1231

1232 El-Sabh, M. I. and Murty, T. S.: Mathematical modelling of tides in the St. Lawrence Estuary, in:
1233 El-Sabh, M. I. and Silverberg, N. (Eds.), *Oceanography of a Large-scale Estuarine System*,
1234 Springer-Verlag, New York, 10-50, 1990.

1235
1236 El-Sabh, M. I. and Silverberg, N.: The St. Lawrence Estuary: introduction, in: El-Sabh, M. I. and
1237 Silverberg, N. (Eds.), *Oceanography of a Large-scale Estuarine System*, Springer-Verlag, New
1238 York, 1-9, 1990.
1239
1240 Frankignoulle, M. et al.: Carbon dioxide emission from European estuaries, *Science*, 282, 434-
1241 436, 1998.
1242
1243 Galbraith, P. S.: Winter water masses in the Gulf of St. Lawrence, *J. Geophys. Res.*, 111, C06022,
1244 doi:10.1029/2005JC003159, 2006.
1245
1246 Gearing, J. N. and Pocklington, R.: Organic geochemical studies in the St. Lawrence Estuary,
1247 in: El-Sabh, M. I. and Silverberg, N. (Eds.), *Oceanography of a Large-scale Estuarine System*,
1248 Springer-Verlag, New York, 170-201, 1990.
1249
1250 Gilbert, D., Sundby, B., Gobeil, C., Mucci, A., and Tremblay, G. H.: A seventy-two-year record
1251 of diminishing deep-water oxygen in the St. Lawrence estuary: The northwest Atlantic
1252 connection, *Limnol. Oceanogr.*, 50, 1654-1666, 2005.
1253
1254 Grasshoff, K., Kremling, K., and Ehrhardt, M. (Eds.): *Methods of Seawater Analysis* (3rd ed.),
1255 Wiley-VCH, Weinheim, Germany, 1999.
1256
1257 Gratton, Y., Mertz, G., and Gagné, J. A.: Satellite observations of tidal upwelling and mixing in
1258 the St. Lawrence Estuary, *J. Geophys. Res.-Oceans*, 93, 6947-6954, 1988.
1259
1260 Hélie, J. F. and Hillaire-Marcel, C.: Sources of particulate and dissolved organic carbon in the
1261 St Lawrence River: isotopic approach, *Hydrol. Process.*, 20, 1945-1959, 2006.
1262
1263 Hélie, J. F., Hillaire-Marcel, C., and Rondeau, B.: Seasonal changes in the sources and fluxes of
1264 dissolved inorganic carbon through the St. Lawrence River—isotopic and chemical constraint,
1265 *Chem. Geol.*, 186, 117-138, 2002.
1266
1267 Ho, D. T., Wanninkhof, R., Schlosser, P., Ullman, D. S., Hebert, D., and Sullivan, K. F.: Toward a
1268 universal relationship between wind speed and gas exchange: Gas transfer velocities
1269 measured with $^3\text{He}/\text{SF}_6$ during the Southern Ocean Gas Exchange Experiment, *J. Geophys.*
1270 *Res.*, 116, C00F04, doi:10.1029/2010JC006854, 2011.
1271

1272 Hunt, C. W., Salisbury, J. E., and Vandemark, D.: Contribution of non-carbonate anions to total
1273 alkalinity and overestimation of pCO₂ in New England and New Brunswick rivers,
1274 *Biogeosciences*, 8, 3069-3076, 2011.
1275
1276 Ingram, R. G. and El-Sabh, M. I.: Fronts and mesoscale features in the St. Lawrence Estuary, in:
1277 El-Sabh, M. I. and Silverberg, N. (Eds.), *Oceanography of a Large-scale Estuarine System*,
1278 Springer-Verlag, New York, 71-93, 1990.
1279
1280 Jiang, L. Q., Cai, W. J., and Wang, Y.: A comparative study of carbon dioxide degassing in river-
1281 and marine-dominated estuaries, *Limnol. Oceanogr.*, 53, 2603-2615, 2008.
1282
1283 Joesoef, A., Huang, W. J., Gao, Y., and Cai, W. J.: Air-water fluxes and sources of carbon
1284 dioxide in the Delaware Estuary: spatial and seasonal variability, *Biogeosciences*, 12, 6085-
1285 6101, 2015.
1286
1287 Kaul, L. W. and Froelich, P. N.: Modeling estuarine nutrient geochemistry in a simple system,
1288 *Geochim. Cosmochim. Acta*, 48, 1417-1433, 1984.
1289
1290 [Koné, Y. J. M., Abril, G., Kouadio, K. N., Delille, B., and Borges, A. V.: Seasonal variability of](#)
1291 [carbon dioxide in the rivers and lagoons of Ivory Coast \(West Africa\), *Estuaries and Coasts*, 32,](#)
1292 [246-260, 2009.](#)
1293
1294 Larouche, P., Koutitonsky, V. G., Chanut, J. P., and El-Sabh, M. I.: Lateral stratification and
1295 dynamic balance at the Matane transect in the lower Saint Lawrence estuary, [Estuar. Coast.](#)
1296 [Shelf Sci.](#), 24, 859-871, 1987.
1297
1298 Laruelle, G. G., Dürr, H. H., Slomp, C. P., and Borges, A. V.: Evaluation of sinks and sources of
1299 CO₂ in the global coastal ocean using a spatially-explicit typology of estuaries and continental
1300 shelves, *Geophys. Res. Lett.*, 37, L15607, doi:10.1029/2010GL043691, 2010.
1301
1302 [Laruelle, G. G., Dürr, H. H., Lauerwald, R., Hartmann, J., Slomp, C. P., Goossens, N., and Regnier,](#)
1303 [P. A. G.: Global multi-scale segmentation of continental and coastal waters from the](#)
1304 [watersheds to the continental margins, *Hydrol. Earth Syst. Sci.*, 17, 2029-2051, 2013.](#)
1305
1306 Laruelle, G. G., Lauerwald, R., Rotschi, J., Raymond, P. A., Hartmann, J., and Regnier, P.:
1307 Seasonal response of air-water CO₂ exchange along the land-ocean aquatic continuum of the
1308 northeast North American coast, *Biogeosciences*, 12, 1447-1458, 2015.

Deleted: .

Deleted: Estuar. Coast. Shelf S.

1311
1312 Lucotte, M.: Organic carbon isotope ratios and implications for the maximum turbidity zone of
1313 the St Lawrence upper estuary, [Estuar. Coast. Shelf Sci.](#), 29, 293-304, 1989.
1314
1315 Lucotte, M. and d'Anglejan, B.: Seasonal control of the Saint-Lawrence maximum turbidity zone
1316 by tidal-flat sedimentation, *Estuaries*, 9, 84-94, 1986.
1317
1318 Lucotte, M., Hillaire-Marcel, C., and Louchouart, P.: First-order organic carbon budget in the
1319 St Lawrence Lower Estuary from ¹³C data, [Estuar. Coast. Shelf Sci.](#), 32, 297-312, 1991.
1320
1321 Lueker, T. J., Dickson, A. G., and Keeling, C. D.: Ocean pCO₂ calculated from dissolved
1322 inorganic carbon, alkalinity, and equations for K₁ and K₂: validation based on laboratory
1323 measurements of CO₂ in gas and seawater at equilibrium, *Mar. Chem.*, 70, 105-119, 2000.
1324
1325 [Maher, D. T., and Eyre, B. D.: Carbon budgets for three autotrophic Australian estuaries:
1326 Implications for global estimates of the coastal air-water CO₂ flux, *Global Biogeochem. Cycles*,
1327 26, GB1032, doi:10.1029/2011GB004075, 2012.](#)
1328
1329 McDougall, T. J. and Barker, P. M.: Getting started with TEOS-10 and the Gibbs Seawater
1330 (GSW) Oceanographic Toolbox, SCOR/IAPSO WG127, ISBN 978-0-646-55621-5, 28 pp., 2011.
1331
1332 Mertz, G. and Gratton, Y.: Topographic waves and topographically induced motions in the St.
1333 Lawrence Estuary, in: El-Sabh, M. I. and Silverberg, N. (Eds.), *Oceanography of a Large-scale
1334 Estuarine System*, Springer-Verlag, New York, 94-108, 1990.
1335
1336 Middelburg, J. J. and Herman, P. M.: Organic matter processing in tidal estuaries, *Mar. Chem.*,
1337 106, 127-147, 2007.
1338
1339 Millero, F. J.: The thermodynamics of the carbonate system in seawater, *Geochim. Cosmochim.*
1340 [Acta](#), 43, 1651-1661, 1979.
1341
1342 Millero, F. J.: The pH of estuarine waters, *Limnol. Oceanogr.*, 31, 839-847, 1986.
1343
1344 Millero, F. J.: Carbonate constants for estuarine waters, *Mar. Freshwater Res.*, 61, 139-142,
1345 2010.
1346

Deleted: Estuar. Coast. Shelf S.

Deleted: Estuar. Coast. Shelf S.

Deleted: .

1350 Monbet, Y.: Control of phytoplankton biomass in estuaries: a comparative analysis of microtidal
1351 and macrotidal estuaries, *Estuaries*, 15, 563-571, 1992.
1352
1353 Mucci, A., Levasseur, M., Gratton, Y., Martias, C., Scarratt, M., Gilbert, D., Tremblay, J.-É.,
1354 Ferreya, G., and Lansard, B.: Tidal-induced variations of pH at the head of the Laurentian
1355 Channel, *Can. J. Fish. Aquat. Sci.* ([in revision](#)), 2016.
1356
1357 Orr, J. C., Epitalon, J. M., and Gattuso, J. P.: Comparison of ten packages that compute ocean
1358 carbonate chemistry, *Biogeosciences*, 12, 1483-1510, 2015.
1359
1360 Painchaud, J. and Therriault, J. C.: Relationships between bacteria, phytoplankton and
1361 particulate organic carbon in the upper St. Lawrence estuary, *Mar. Ecol.-Prog. Ser.*, 56, 301-
1362 311, 1989.
1363
1364 Painchaud, J., Lefavre, D., Therriault, J. C., and Legendre, L.: Physical processes controlling
1365 bacterial distribution and variability in the upper St. Lawrence estuary, *Estuaries*, 18, 433-444,
1366 1995.
1367
1368 Pelletier, E. and Lebel, J.: Hydrochemistry of dissolved inorganic carbon in the St. Lawrence
1369 Estuary (Canada), *Estuar. Coast. Mar. Sci.*, 9, 785-795, 1979.
1370
1371 Peng, T. H., Takahashi, T., Broecker, W. S., and Olafsson, J.: Seasonal variability of carbon
1372 dioxide, nutrients and oxygen in the northern North Atlantic surface water: observations and a
1373 model, *Tellus*, 39B, 439-458, 1987.
1374
1375 Plourde, S. and Runge, J. A.: Reproduction of the planktonic copepod *Calanus finmarchicus* in
1376 the Lower St. Lawrence Estuary: relation to the cycle of phytoplankton production and
1377 evidence for a *Calanus* pump, *Mar. Ecol.-Prog. Ser.*, 102, 217-227, 1993.
1378
1379 Pocklington, R. and Leonard, J. D.: Terrigenous organic matter in sediments of the St. Lawrence
1380 Estuary and the Saguenay Fjord, *J. Fish. Res. Board Can.*, 36, 1250-1255, 1979.
1381
1382 Poisson, A., Metzl, N., Brunet, C., Schauer, B., Bres, B., Ruiz-Pino, D., and Louanchi, F.: Variability
1383 of sources and sinks of CO₂ in the Western Indian and Southern Oceans during the year 1991,
1384 *J. Geophys. Res.-Oceans*, 98, 22759-22778, 1993.
1385

Deleted: submitted

Deleted: Discussions

1388 Raymond, P. A. and Cole, J. J.: Gas exchange in rivers and estuaries: Choosing a gas transfer
1389 velocity, *Estuaries*, 24, 312-317, 2001.
1390
1391 Raymond, P. A., Bauer, J. E., and Cole, J. J.: Atmospheric CO₂ evasion, dissolved inorganic
1392 carbon production, and net heterotrophy in the York River estuary, *Limnol. Oceanogr.*, 45,
1393 1707-1717, 2000.
1394
1395 Regnier, P. et al.: Anthropogenic perturbation of the carbon fluxes from land to ocean, *Nat.*
1396 *Geosci.*, 6, 597-607, 2013.
1397
1398 Richey, J. E., Devol, A. H., Wofsy, S. C., Victoria, R., and Riberio, M. N.: Biogenic gases and the
1399 oxidation and reduction of carbon in Amazon River and floodplain waters, *Limnol. Oceanogr.*,
1400 33, 551-561, 1988.
1401
1402 Robert-Baldo, G. L., Morris, M. J., and Byrne, R. H.: Spectrophotometric determination of
1403 seawater pH using phenol red, *Anal. Chem.*, 57, 2564-2567, 1985.
1404
1405 Roy, R. N. et al.: The dissociation constants of carbonic acid in seawater at salinities 5 to 45 and
1406 temperatures 0 to 45°C, *Mar. Chem.*, 44, 249-267, 1993.
1407
1408 Saucier, F. J. and Chassé, J.: Tidal circulation and buoyancy effects in the St. Lawrence Estuary,
1409 *Atmos. Ocean*, 38, 505-556, 2000.
1410
1411 Saucier, F. J., Roy, F., Gilbert, D., Pellerin, P., and Ritchie, H.: Modeling the formation and
1412 circulation processes of water masses and sea ice in the Gulf of St. Lawrence, Canada. *J.*
1413 *Geophys. Res.*, 108, 3269, doi:10.1029/2000JC000686, 2003.
1414
1415 Savenkoff, C., Comeau, L., Vézina, A. F., and Gratton, Y.: Seasonal variation of the biological
1416 activity in the lower St. Lawrence Estuary, *Can. Tech. Rep. Fish. Aquat. Sci.*, 2006, 22 pp., 1994.
1417
1418 Silverberg, N. and Sundby, B.: Observations in the turbidity maximum of the St. Lawrence
1419 estuary, *Can. J. Earth Sci.*, 16, 939-950, 1979.
1420
1421 Sprintall, J. and Tomczak, M.: Evidence of the barrier layer in the surface layer of the tropics, *J.*
1422 *Geophys. Res.-Oceans*, 97, 7305-7316, 1992.
1423

Deleted: Estuar. Coast.

1425 Statham, P. J.: Nutrients in estuaries—an overview and the potential impacts of climate change,
1426 *Sci. Total Environ.*, 434, 213-227, 2012.
1427
1428 Takahashi, T., Olafsson, J., Goddard, J. G., Chipman, D. W., and Sutherland, S. C.: Seasonal
1429 variation of CO₂ and nutrients in the high-latitude surface oceans: a comparative study, *Global*
1430 *Biogeochem. Cycles*, 7, 843-878, 1993.
1431
1432 Takahashi, T. et al.: Global sea-air CO₂ flux based on climatological surface ocean pCO₂, and
1433 seasonal biological and temperature effects, *Deep-Sea Res. Pt. II*, 49, 1601-1622, 2002.
1434
1435 Tan, F. C. and Strain, P. M.: Sources, sinks and distribution of organic carbon in the St. Lawrence
1436 Estuary, Canada, *Geochim. Cosmochim. Acta*, 47, 125-132, 1983.
1437
1438 Tee, K-T.: Meteorologically and buoyancy induced subtidal salinity and velocity variations in
1439 the St. Lawrence Estuary, in: El-Sabh, M. I. and Silverberg, N. (Eds.), *Oceanography of a Large-*
1440 *scale Estuarine System*, Springer-Verlag, New York, 51-70, 1990.
1441
1442 Uncles, R. J., Stephens, J. A., and Smith, R. E.: The dependence of estuarine turbidity on tidal
1443 intrusion length, tidal range and residence time, *Cont. Shelf Res.*, 22, 1835-1856, 2002.
1444
1445 van Heuven, S., Pierrot, D., Rae, J. W. B., Lewis, E., and Wallace, D. W. R.: MATLAB program
1446 developed for CO₂ system calculations, ORNL/CDIAC-105b, Carbon Dioxide Information
1447 Analysis Center, Oak Ridge National Laboratory, U.S. Department of Energy, Oak Ridge,
1448 Tennessee, doi: 10.3334/CDIAC/otg.CO2SYS_MATLAB_v1.1, 2011.
1449
1450 Wanninkhof, R.: Relationship between wind speed and gas exchange over the ocean, *J.*
1451 *Geophys. Res.-Oceans*, 97, 7373-7382, 1992.
1452
1453 Wanninkhof, R.: Relationship between wind speed and gas exchange over the ocean revisited,
1454 *Limnol. Oceanogr.-Meth.*, 12, 351-362, 2014.
1455
1456 Weiss, R.: Carbon dioxide in water and seawater: the solubility of a non-ideal gas, *Mar. Chem.*,
1457 2, 203-215, 1974.
1458
1459 Weiss, R. F. and Price, B. A.: Nitrous oxide solubility in water and seawater, *Mar. Chem.*, 8, 347-
1460 359, 1980.
1461

Deleted: .

Deleted: .

1464 Working Group on the State of the St. Lawrence Monitoring, Overview of the State of the St.
1465 Lawrence 2014, St. Lawrence Action Plan, Environment Canada, Québec's ministère du
1466 Développement durable, de l'Environnement et de la Lutte contre les changements
1467 climatiques), Québec's ministère des Forêts, de la Faune et des Parcs, Parks Canada, Fisheries
1468 and Oceans Canada, and Stratégies Saint-Laurent, 52 pp., 2014.
1469
1470 Yang, B., Byrne, R. H., and Lindemuth, M.: Contributions of organic alkalinity to total alkalinity
1471 in coastal waters: A spectrophotometric approach, *Mar. Chem.*, 176, 199-207, 2015.
1472
1473 Yang, C., Telmer, K., and Veizer, J.: Chemical dynamics of the "St. Lawrence" riverine system:
1474 δD_{H_2O} , $\delta^{18}O_{H_2O}$, $\delta^{13}C_{DIC}$, $\delta^{34}S_{sulfate}$, and dissolved $^{87}Sr/^{86}Sr$, *Geochim. Cosmochim. Acta*, 60, 851-
1475 866, 1996.
1476
1477 Yeats, P. A.: Reactivity and transport of nutrients and metals in the St. Lawrence Estuary, in: El-
1478 Sabh, M. I. and Silverberg, N. (Eds.), *Oceanography of a Large-scale Estuarine System*,
1479 Springer-Verlag, New York, 155-169, 1990.
1480
1481 Zakardjian, B. A., Gratton, Y., and Vézina, A. F.: Late spring phytoplankton bloom in the Lower
1482 St. Lawrence Estuary: the flushing hypothesis revisited, *Mar. Ecol.-Prog. Ser.*, 192, 31-48, 2000.
1483
1484 Zappa, C. J., Raymond, P. A., Terray, E. A., and McGillis, W. R.: Variation in surface turbulence
1485 and the gas transfer velocity over a tidal cycle in a macro-tidal estuary, *Estuaries*, 26, 1401-
1486 1415, 2003.
1487
1488 Zappa, C. J., McGillis, W. R., Raymond, P. A., Edson, J. B., Hints, E. J., Zemmelen, H. J., Dacey,
1489 J. W. H., and Ho, D. T.: Environmental turbulent mixing controls on air-water gas exchange in
1490 marine and aquatic systems, *Geophys. Res. Lett.*, 34, L10601, doi:10.1029/2006GL028790,
1491 2007.
1492
1493
1494
1495
1496
1497
1498
1499
1500

Deleted: .

1502 **Table 1.** Mean, standard deviation and range of the surface-water temperature (T),
 1503 practical salinity (S_p), dissolved inorganic carbon (DIC), total alkalinity (TAlk) and *in situ*
 1504 partial pressure of CO_2 (pCO_2) in the St. Lawrence River (near Québec City), Upper
 1505 Estuary (Île d'Orléans to Tadoussac), Lower Estuary (Tadoussac to Pointe-des-Monts)
 1506 and Gulf (Pointe-des-Monts to Cabot Strait) during all sampling months.

	T (°C)	S_p	DIC ($\mu mol\ kg^{-1}$)	TAlk ($\mu mol\ kg^{-1}$)	pCO_2 (μatm)
River (N=3)	14.2 ± 3.9 (9.8-17.2)	0.03 ± 0.05 (0-0.09)	1242 ± 132 (1148-1335)	1204 ± 99 (1124-1314)	604 ± 76 (550-658)
Upper (N=46)	9.6 ± 3.6 (4.2-17.4)	10.9 ± 8.0 (0-24.5)	1514 ± 242 (1081-2005)	1492 ± 272 (969-2030)	571 ± 72 (435-765)
Lower (N=60)	6.2 ± 2.2 (2.7-12.6)	26.2 ± 2.1 (21.2-30.4)	1837 ± 82 (1634-2005)	1957 ± 82 (1752-2088)	394 ± 119 (139-578)
Gulf (N=30)	8.8 ± 3.1 (3.9-13.7)	30.1 ± 1.5 (25.5-31.5)	1936 ± 64 (1761-2032)	2096 ± 61 (1921-2175)	352 ± 80 (207-478)

Deleted: -
Deleted: -

Deleted: 5.6
 Deleted: 8
 Deleted: 8
 Deleted: 7
 Deleted: 43
 Deleted: 9
 Deleted: 62
 Deleted: 7
 Deleted: 7
 Deleted: -0.32
 Deleted: 2
 Deleted: 7
 Deleted: 83
 Deleted: 185
 Deleted: 4
 Deleted: 4
 Deleted: 2

1507
 1508
 1509
 1510
 1511
 1512
 1513
 1514
 1515
 1516
 1517
 1518
 1519
 1520
 1521
 1522
 1523
 1524
 1525

1545 **Table 2.** Mean, standard deviation and range of $\Delta p\text{CO}_2$, k_{W-14} , $k_{R\&C-01}$, F_{W-14} and $F_{R\&C-01}$
 1546 in the surface waters of the St. Lawrence River, Upper Estuary, Lower Estuary and Gulf
 1547 during all sampling months. k_{W-14} are the gas transfer velocities given by the
 1548 Wanninkhof (2014) relationship, whereas $k_{R\&C-01}$ are those given by Raymond and Cole
 1549 (2001). Values of F_{W-14} are taken to be the theoretical lower limit of air-sea gas
 1550 exchange, whereas values of $F_{R\&C-01}$ are the upper limit; the extreme F data points are
 1551 shown in bold.

	$\Delta p\text{CO}_2$ (μatm)	k_{W-14} (cm h^{-1})	$k_{R\&C-01}$ (cm h^{-1})	F_{W-14} ($\text{mmol m}^{-2} \text{d}^{-1}$)	$F_{R\&C-01}$ ($\text{mmol m}^{-2} \text{d}^{-1}$)
River (N=3)	217 ± 99 (147-287)	3.0 ± 1.4 (1.9-4.5)	6.1 ± 2.0 (4.3-8.2)	5.8 ± 3.2 (3.5-8.0)	12.7 ± 6.4 (8.2- 17.3)
Upper (N=46)	184 ± 72 (43-386)	2.8 ± 0.8 (1.6-4.5)	5.6 ± 1.1 (3.8-8.1)	6.1 ± 3.0 (2.0-14.7)	12.3 ± 5.4 (3.6- 28.4)
Lower (N=60)	9.2 ± 11.6 (-266-188)	3.2 ± 0.4 (2.0-3.8)	5.9 ± 0.6 (4.3-6.9)	0.6 ± 4.9 (-12.1-8.3)	1.0 ± 9.0 (-21.9-15.1)
Gulf (N=30)	-31.0 ± 9.0 (-178-107)	1.2 ± 0.3 (0.8-1.7)	3.4 ± 0.3 (2.8-4.1)	-0.8 ± 1.5 (-3.6-1.1)	-1.7 ± 3.9 (-8.4-3.6)

- Deleted: -
- Deleted: -
- Deleted: -
- Deleted: -
- Deleted: -
- Deleted: 8.7
- Deleted: 5
- Deleted: 5
- Deleted: 8
- Deleted: 8.9
- Deleted: 28.4
- Deleted: 1
- Deleted: 7
- Deleted: 6

1552
 1553
 1554
 1555
 1556
 1557
 1558
 1559
 1560
 1561
 1562
 1563
 1564
 1565
 1566
 1567

1583 **Table 3.** Sectional and area-averaged air-sea CO₂ fluxes (mmol C m⁻² d⁻¹) in the St.
 1584 Lawrence Estuary during all sampling months. To obtain the area-averaged CO₂ flux,
 1585 the SLE was divided into five segments at equal intervals. The first row of the table
 1586 shows the surface area (km²) of each segment. The flux data in each segment were
 1587 numerically averaged to obtain sectional fluxes, which were then area weighted and
 1588 summed to obtain the spatially integrated whole-estuary flux (in bold). The F_{W-14} and
 1589 F_{R&C-01} data provide the lower and upper estimates, respectively.

	Seg 1 (N=17)	Seg 2 (N=23)	Seg 3 (N=21)	Seg 4 (N=17)	Seg 5 (N=8)	Whole estuary
Surface area (km ²)	1,098	2,250	2,726	3,404	3,303	12,781
F _{W-14} (mmol m ⁻² d ⁻¹)	7.2	5.4	4.3	-1.8	-4.0	0.98
F _{R&C-01} (mmol m ⁻² d ⁻¹)	14.5	11.0	7.9	-3.5	-7.4	2.02

1590
1591
1592
1593
1594
1595
1596
1597
1598
1599
1600
1601
1602
1603
1604
1605
1606
1607
1608
1609
1610
1611
1612

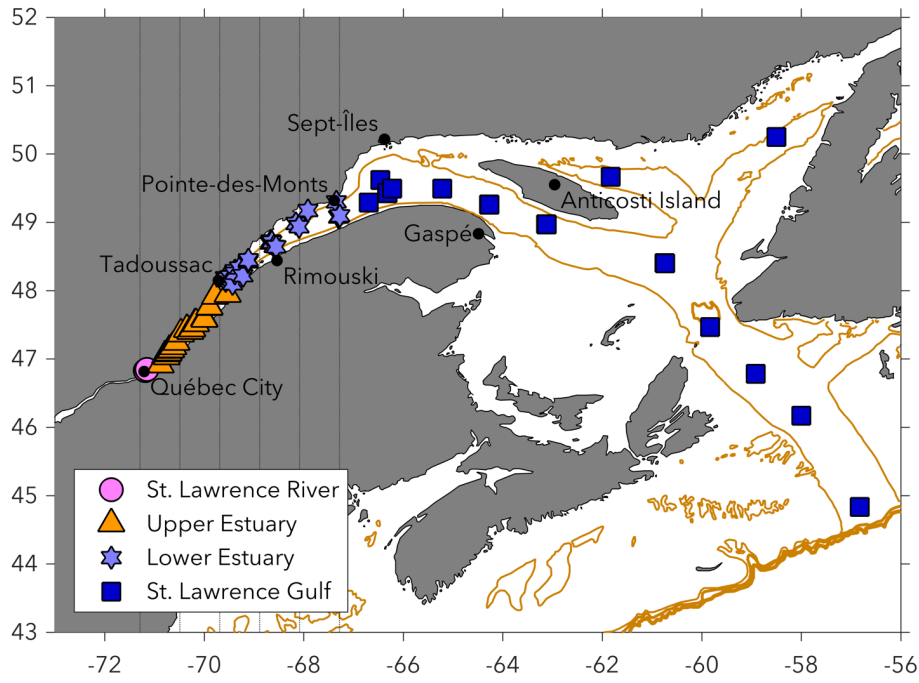
Deleted: -
Deleted: -

Deleted: -
Deleted: -
Deleted: 7
Deleted: **1.00**
Deleted: -
Deleted: -
Deleted: 3
Deleted: **2.06**



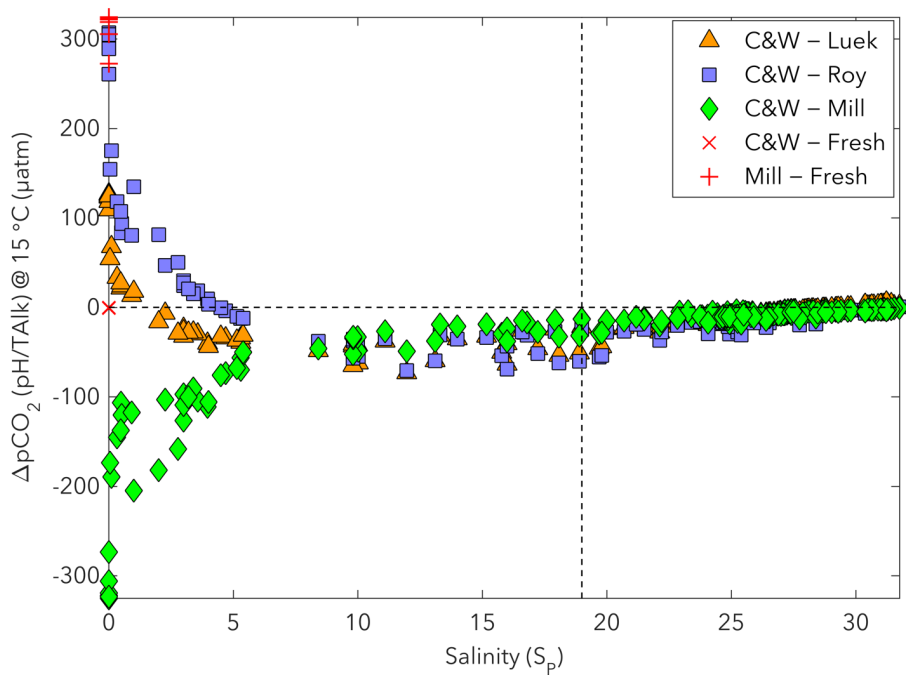
1623
 1624 **Figure 1.** Map of the greater St. Lawrence system, including the chain of Great Lakes,
 1625 the St. Lawrence River, the Upper St. Lawrence Estuary (USLE), the Lower St. Lawrence
 1626 Estuary (LSLE), and the Gulf of St. Lawrence (GSL). From: Overview of the State of the
 1627 St. Lawrence 2014 (with permission).

1628
 1629
 1630
 1631
 1632
 1633
 1634
 1635
 1636
 1637
 1638
 1639
 1640
 1641
 1642



1643
1644
1645
1646
1647
1648
1649
1650
1651
1652
1653
1654
1655
1656
1657
1658

Figure 2. Map showing the four principal subdivisions of the study area and the sampling locations (markers). Water samples were collected during ten spring/summer research cruises: July 2003, June 2006, May 2007, July 2007, June 2009, July 2009, July 2010, May 2011, June 2013 and May 2016. The estuary, from the landward limit of the salt water intrusion near Île d'Orléans (~5 km downstream of Québec City) to Pointe-des-Monts, where the coastline diverges, extends ~400 km and covers a total surface area of ~12,820 km². The solid gold line follows the 200m isobath of the Laurentian Channel. The vertical dotted lines delineate the five segments of the estuary used for the calculation of the area-averaged CO₂ flux.

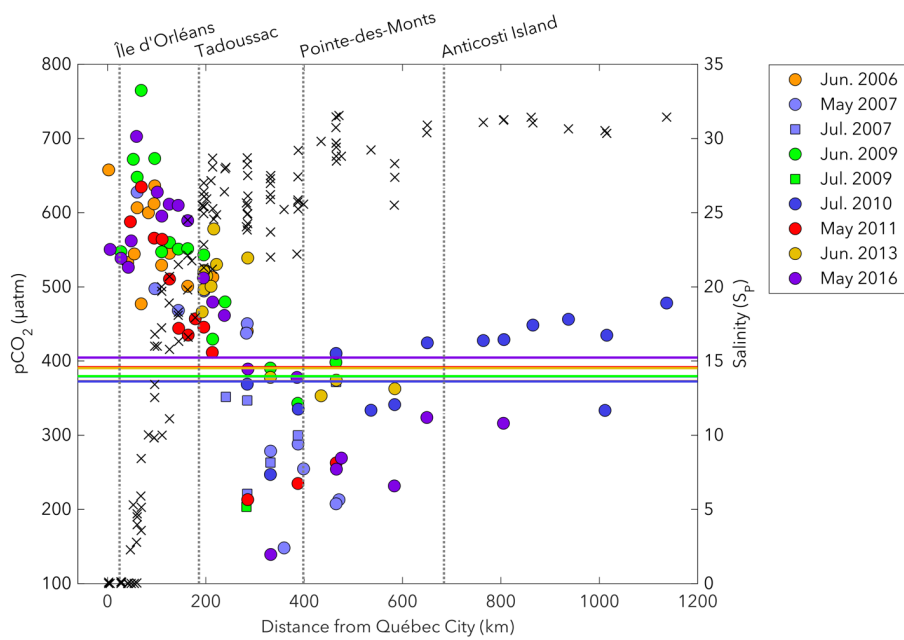


Formatted: Font:Avenir Next

1659
 1660 **Figure 3.** Differences in $p\text{CO}_2$ ($\Delta p\text{CO}_2$) calculated using different published
 1661 formulations of K_1 and K_2 , including Cai and Wang (1998) [C&W], Lueker et al. (2000)
 1662 [Luek], Roy et al. (1993) [Roy], Millero (2010) [Mill], and Millero (1979) for pure water
 1663 only ($S_p = 0$) [Fresh]. All calculations were carried out at 15 °C ($p\text{CO}_2$ @ 15 °C) with
 1664 measured pH and TAlk. The constants of Lueker et al. (2000) are recommended for
 1665 best practices by Dickson et al. (2007), whereas those of Roy et al. (1993) ($S_p = 5$ to 45)
 1666 are recommended by Dickson and Goyet (1994). Both the constants of Cai and Wang
 1667 (1998) and Millero (2010) have been proposed as more appropriate for the study of
 1668 the carbonate system in estuarine waters.

Deleted: of
 Deleted: from measured pH and TAlk with

1669
 1670
 1671
 1672
 1673
 1674



Formatted: Font:Avenir Next Demi Bold, Bold

1677

1678 **Figure 4.** Spatial distributions of surface-water pCO₂ (circles, squares) and practical
 1679 salinity (x symbols) in the St. Lawrence River, Estuary and Gulf during spring/summer
 1680 cruises. Horizontal lines show the mean pCO₂(air) in the sampling months. The pCO₂
 1681 data points above atmospheric level are sources of CO₂ to the atmosphere whereas
 1682 those below atmospheric level are sinks of atmospheric CO₂.

1683

1684

1685

1686

1687

1688

1689

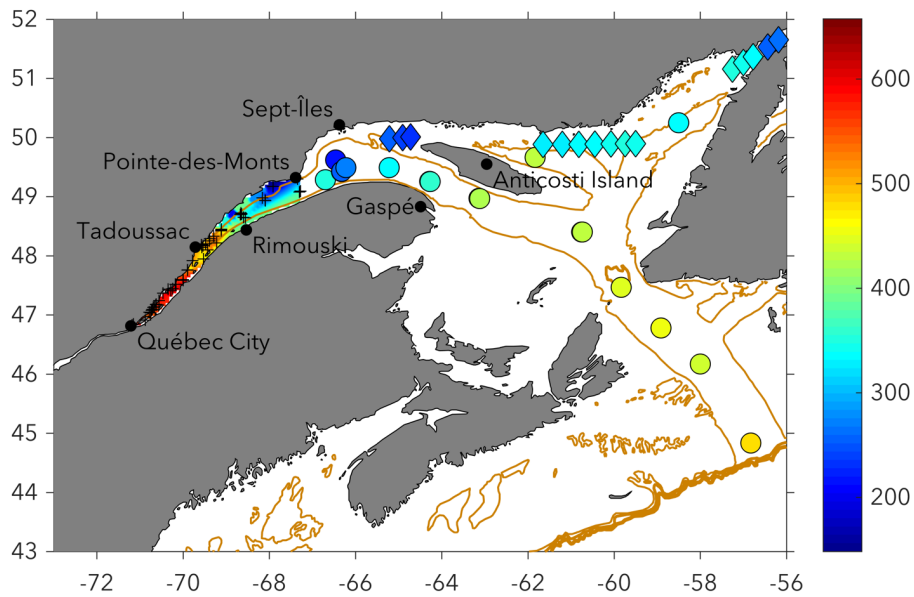
1690

1691

1692

1693

Formatted: Not Superscript/ Subscript



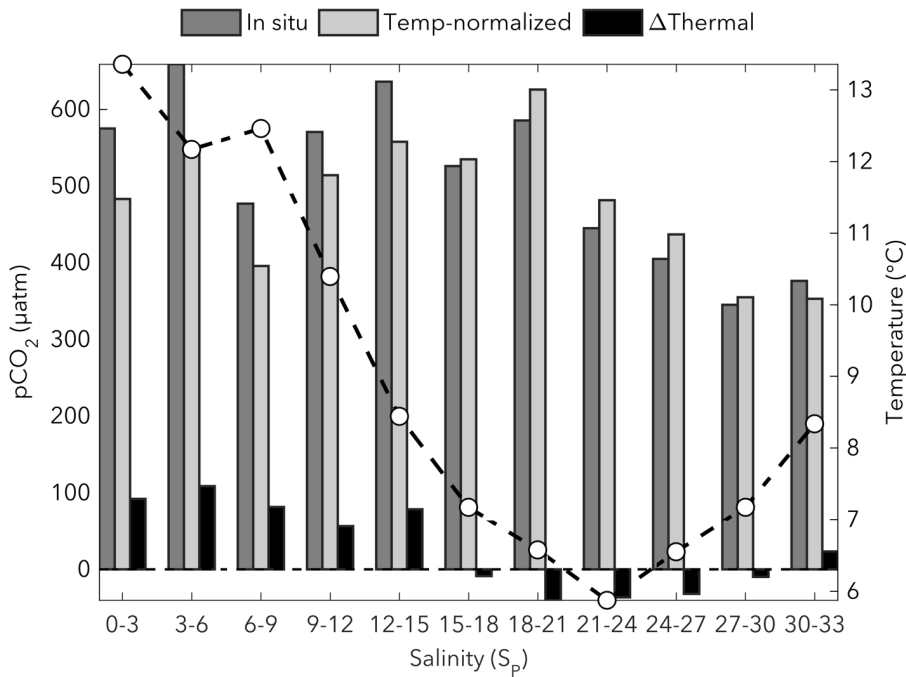
1694
 1695 **Figure 5.** Spatial distribution of surface-water pCO₂ (µatm) in the St. Lawrence Estuary
 1696 and Gulf during all spring/summer cruises. Linear interpolation was used between the
 1697 sampling locations in the estuary (+ symbols). Circles show calculated pCO₂ (pH/TALK),
 1698 whereas diamonds show pCO₂ measured by the underway system (General Oceanics
 1699 model 8050) aboard the CCGS *Amundsen* in June 2016 (Dr. Tim
 1700 Papakyriakou/University of Manitoba, pers. comm.). For neighboring locations
 1701 sampled in May 2016 aboard the RV *Coriolis II*, measured and calculated pCO₂ differed
 1702 by, on average, ~4.2 %. The mean atmospheric pCO₂ during the sampling months
 1703 ranged from 372 to 405 µatm.

Formatted: Font:Avenir Next

Deleted: in the estuary

Formatted: Font:Italic

Deleted: Linear interpolation was used between the sampling locations (+ symbols).



1715
1716
1717
1718
1719
1720
1721
1722
1723
1724
1725
1726
1727
1728

Figure 6. Surface-water *in situ* pCO_2 , temperature-normalized pCO_2 , and $\Delta pCO_2(TEMP)$ averaged over salinity bins of 3. The open circles show the average temperature for each salinity bin. To correct for the increasing/decreasing effect of temperature on surface-water pCO_2 , the *in situ* pCO_2 were normalized to the average surface-water temperature of the study area ($T = 7.82^{\circ}C$). The $\Delta pCO_2(TEMP)$ are the thermally-induced pCO_2 changes due to temperature deviations from $T = 7.82^{\circ}C$, whereas variations in temperature-normalized pCO_2 are due to water mass mixing and/or biological activity.

Formatted: Font:Avenir Next

Deleted: The s

Deleted: hermal

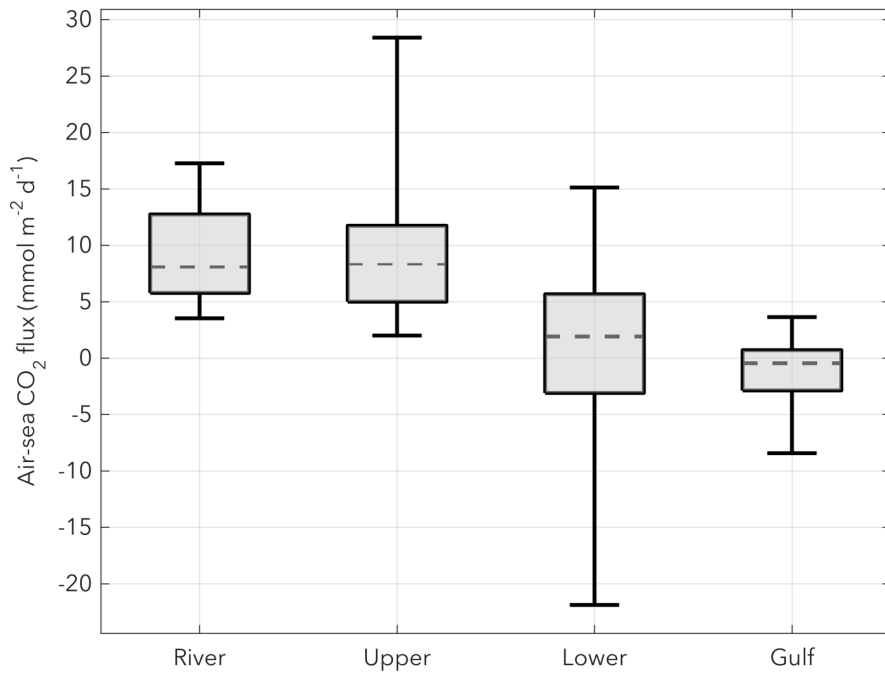
Formatted: Not Superscript/ Subscript

Formatted: Not Superscript/ Subscript

Formatted: Not Superscript/ Subscript

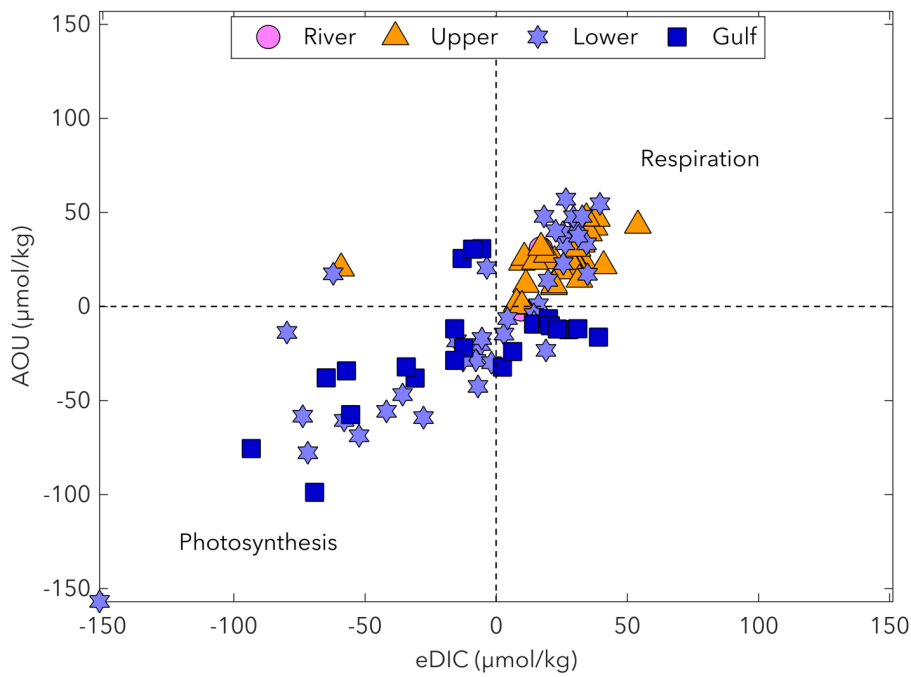
Deleted: hermal

Formatted: Not Superscript/ Subscript



1732
1733
1734
1735
1736
1737
1738
1739
1740
1741
1742
1743
1744
1745

Figure 7. Box plot showing the variability of air-sea CO₂ fluxes in the four principal subdivisions of the study area (St. Lawrence River, Upper Estuary, Lower Estuary and Gulf). The box spans the interquartile range (25-75 percentiles), the dashed line is the median, and the whiskers extend to the extreme data points. The F_{W-14} data were combined with the F_{R&C-01} data from all spring/summer sampling months to depict the upper and lower limits of gas exchange.



Formatted: Font:Avenir Next Demi Bold, Bold

1747
1748
1749
1750
1751
1752
1753
1754
1755
1756
1757
1758
1759
1760
1761
1762

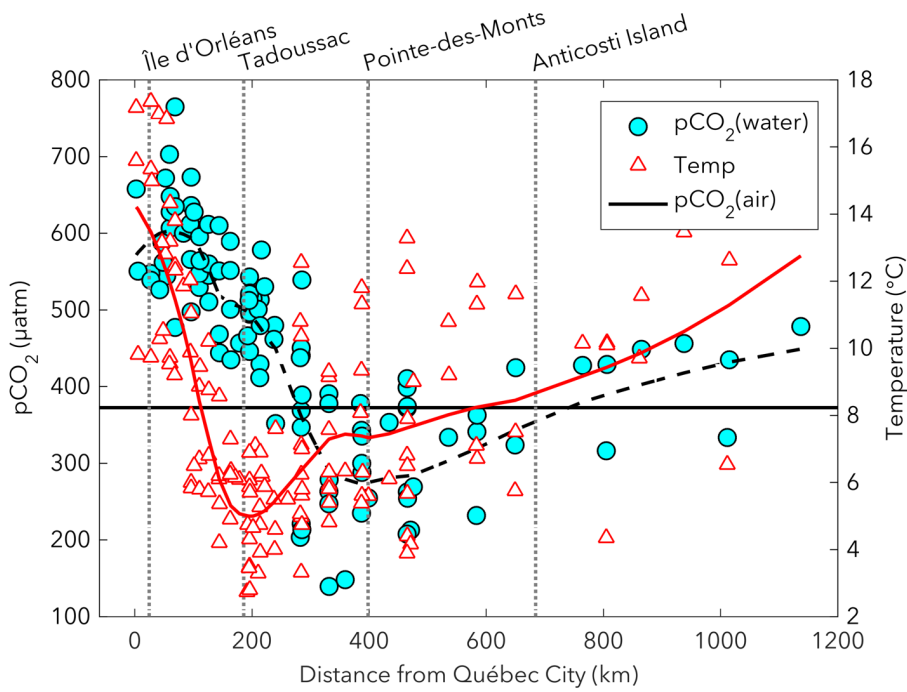
Figure 8. Top: comparison of the saturation states (or % saturation) of pCO₂ and DO in the mixed-layer waters of the St. Lawrence River, Estuary and Gulf. Dashed lines delineate the 100 % saturation levels for both gases. Surface-water samples (markers) fall into one of four quadrants representing the dominant controls on CO₂/O₂ dynamics. Quadrants I and III indicate the effects of photosynthesis/respiration, whereas Quadrants II and IV indicate heating/cooling. Bottom: comparison of the apparent oxygen utilization (AOU) and excess DIC (eDIC). Respiration/remineralization processes are reflected in positive values of AOU and eDIC, whereas the effects of photosynthesis are reflected in negative values.

Deleted: C

Deleted: surface

Deleted:

Deleted: the effects of



1767
 1768 **Figure 9.** Spatial distributions of surface-water pCO₂ (circles) and temperature
 1769 (triangles) in the St. Lawrence River, Estuary and Gulf during spring/summer cruises.
 1770 Temperatures ranged from 4.2 to 17.4 °C (generally decreasing) in the USLE, 2.7 to
 1771 12.6 °C (generally increasing) in the LSLE, and 3.9 to 13.7 °C (generally increasing) in
 1772 the GSL. The horizontal line shows the mean atmospheric pCO₂, pCO₂(air), during all
 1773 sampling months. The dashed line is the smoothed pCO₂(water) data using a moving
 1774 average filter with a span of 50% of the total number of data points, whereas the red
 1775 line is the smoothed temperature data.

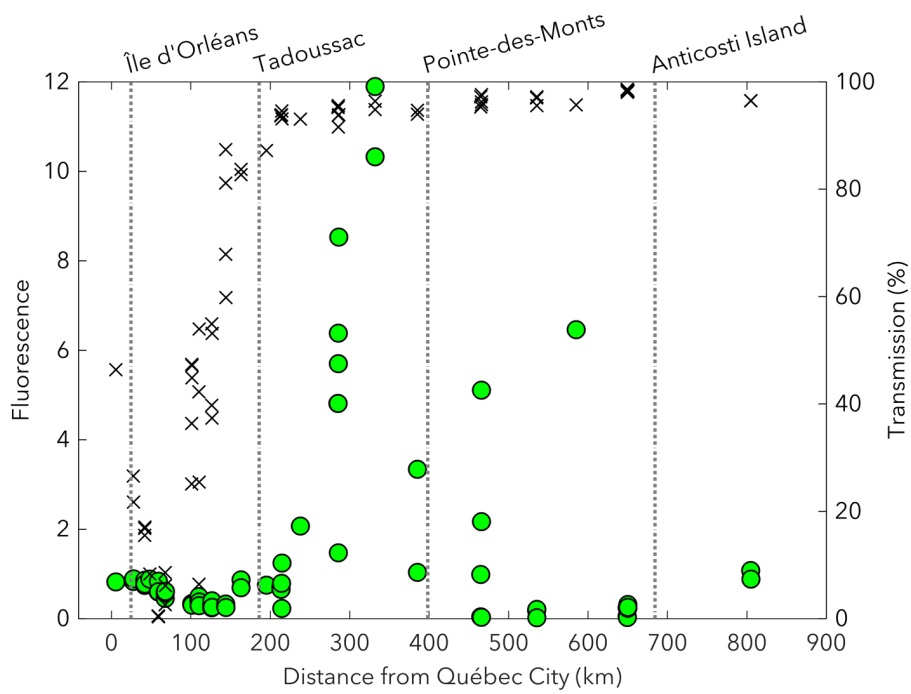
Formatted: Font:Avenir Next

Deleted: diamonds

Deleted: -0.32

Formatted: Not Superscript/ Subscript

1776
 1777
 1778
 1779
 1780
 1781
 1782



Formatted: Font:Avenir Next

1785
1786
1787
1788
1789
1790
1791

Figure 10. Spatial distributions of maximum fluorescence values (circles) and mean transmission values (x symbols) in the euphotic zone of the St. Lawrence River, Estuary and Gulf during the May 2016 cruise. Fluorescence is a primary production proxy, whereas transmission is an excellent proxy for turbidity (low transmission values are due to light absorption by suspended particulate matter and/or colored dissolved organic matter).

variability

Page 19: [1] Deleted **Microsoft Office User** **4/28/17 4:21:00 PM**

variability

Page 19: [1] Deleted **Microsoft Office User** **4/28/17 4:21:00 PM**

variability

Page 19: [1] Deleted **Microsoft Office User** **4/28/17 4:21:00 PM**

variability

Page 19: [1] Deleted **Microsoft Office User** **4/28/17 4:21:00 PM**

variability

Page 19: [1] Deleted **Microsoft Office User** **4/28/17 4:21:00 PM**

variability

Page 19: [1] Deleted **Microsoft Office User** **4/28/17 4:21:00 PM**

variability

Page 19: [1] Deleted **Microsoft Office User** **4/28/17 4:21:00 PM**

variability

Page 19: [1] Deleted **Microsoft Office User** **4/28/17 4:21:00 PM**

variability

Page 19: [2] Deleted **Microsoft Office User** **4/20/17 5:31:00 PM**

To obtain an area-averaged CO₂ flux for the whole estuar

Page 19: [2] Deleted **Microsoft Office User** **4/20/17 5:31:00 PM**

To obtain an area-averaged CO₂ flux for the whole estuar

Page 19: [2] Deleted **Microsoft Office User** **4/20/17 5:31:00 PM**

To obtain an area-averaged CO₂ flux for the whole estuar

Page 19: [2] Deleted **Microsoft Office User** **4/20/17 5:31:00 PM**

To obtain an area-averaged CO₂ flux for the whole estuar

Page 19: [2] Deleted **Microsoft Office User** **4/20/17 5:31:00 PM**

To obtain an area-averaged CO₂ flux for the whole estuar

Page 19: [2] Deleted **Microsoft Office User** **4/20/17 5:31:00 PM**

To obtain an area-averaged CO₂ flux for the whole estuar

Page 19: [2] Deleted **Microsoft Office User** **4/20/17 5:31:00 PM**

To obtain an area-averaged CO₂ flux for the whole estuar

To obtain an area-averaged CO₂ flux for the whole estuar

Page 19: [2] Deleted	Microsoft Office User	4/20/17 5:31:00 PM
----------------------	-----------------------	--------------------

To obtain an area-averaged CO₂ flux for the whole estuar

Page 19: [2] Deleted	Microsoft Office User	4/20/17 5:31:00 PM
----------------------	-----------------------	--------------------

To obtain an area-averaged CO₂ flux for the whole estuar

Page 19: [2] Deleted	Microsoft Office User	4/20/17 5:31:00 PM
----------------------	-----------------------	--------------------

To obtain an area-averaged CO₂ flux for the whole estuar

Page 20: [3] Deleted	Microsoft Office User	4/15/17 7:03:00 PM
----------------------	-----------------------	--------------------

variations in pCO₂ due to water mass mixing and those due to *in situ* biological activity

Page 20: [4] Deleted	Microsoft Office User	4/17/17 3:18:00 PM
----------------------	-----------------------	--------------------

effects of photosynthesis and temperature predominated in